

Strontium Isotopic and Micropalaeontological Dating Used to Help Redefine the Stratigraphy of the Neotectonic Hatay Graben, Southern Turkey

SARAH J. BOULTON^{1,2}, ALASTAIR H.F. ROBERTSON¹,
ROBERT M. ELLAM³, ÜMİT ŞAFAK⁴ & ULVİ CAN ÜNLÜGENÇ⁴

¹ School of GeoSciences, Grant Institute, Edinburgh University, Edinburgh, EH9 3JW, UK

² Now at the School of Earth, Ocean and Environmental Sciences, University of Plymouth, Drake Circus, Plymouth, Devon, PL4 8AA, UK (e-mail: sarah.boulton@plymouth.ac.uk)

³ SUERC, Rankine Avenue, Scottish Enterprise Technology Park, East Kilbride, G75 0QF, UK

⁴ Department of Geological Engineering, Çukurova University, Balcalı, TR-01330 Adana, Turkey

Abstract: In this paper we report for the Hatay Graben, new micropalaeontology, the first strontium dating and new sedimentology. The previous lack of a modern systematic stratigraphy was problematic for the study of the Hatay region. With the new data combined with the existing literature we evaluate and redefine the lithostratigraphy following international standards. The focus of this paper is on the Neogene cover rocks that record the transition from a regional carbonate shelf environment during Palaeocene to Eocene times, through late-stage continental collision, to recent continental rift tectonics that were initiated in the Middle Miocene and continue to operate to the present-day.

The Eocene–Pliocene sedimentary cover of the Hatay Graben is here divided into six formations and one member; Samandağı Formation (Pliocene), Vakıflı Member (Messinian), Nurzeytin Formation (Serravalian–Tortonian, ~13.2–8.6 Ma), Sofular Formation (Burdigalian–Langian), Balyatağı Formation (Aquitaniyan–Burdigalian), Kışlak Formation (Eocene), and Okçular Formation (Eocene). Similar sediments of the Karasu Rift are termed the Gökdere Formation (Tortonian–Messinian), Kepez Formation (Langian), Kıcı Formation (Burdigalian), and Hacıdağı Formation (Palaeocene–Eocene). A brief interpretation of the stratigraphical relationships is also given.

Key Words: Cenozoic stratigraphy, strontium isotopes, micropalaeontology, Hatay Graben, Karasu Rift, Dead Sea Fault Zone, Eastern Mediterranean

Neotektonik Hatay Grabeninin Senozoyik Stratigrafisini Yeniden Belirlemek Üzere Stronsiyum İzotop ve Mikropaleontolojik Verilerle Yaşlandırılması, Güney Türkiye

Özet: Güney Türkiye'deki Hatay bölgesinde ortaya konulan stratigrafi eksik ve problemlidir. Ölü Deniz Fay Zonu, Doğu Anadolu Fay Zonu ve Kıbrıs yayı arasında aktif olarak deformasyon geçiren kıtasal kabuğun bulunduğu alanın tektonik önemi ve son günlerde çalışma bölgesi üzerine oluşan ilgi dolayısıyla, bölgedeki Neojen sedimanter istifin yeniden belirlenerek litostratigrafik adlamasının standartlaşması gerekmektedir. Bu inceleme, mikropaleontolojik ve ilk olarak yapılan stronsiyum yaşlandırılması ile yeni saha verilerinin kullanılması ve önceki çalışmaların yeniden gözden geçirilmesi şeklinde güney Türkiye'deki Hatay bölgesinde yapılan çalışmayı ortaya koymaktadır. Bu çalışmada aynı zamanda bölgenin sedimentolojisi de ortaya konmaktadır. Bölgedeki Neojen yaşlı sedimanlar, bu çalışmada yeniden tanımlanmayacak olan Geç Kretase döneminde bölgeye yerleşen Kızıldağ Ofiyolitlerini üzerler. Bu çalışmanın ilgi odağı, kıtasal çarpışmanın geç dönemi boyunca Paleosen'den Eosen dönemi boyunca gelişen bölgesel karbonat şelf ortamından, Orta Miyosen'de başlayıp günümüze kadar süregelen güncel kıtasal açılma tektoniğinin izlerini taşıyan döneme kadar olan Neojen yaşlı örtü kayalarını kapsamaktadır. Hatay grabenindeki Eosen–Pliyosen yaşlı sedimanter örtü, altı formasyon ve bir üyeye ayrılmıştır. Bunlar: Samandağ Formasyonu (Pliyosen), Vakıflı üyesi (Messiniyen), Nurzeytin Formasyonu (Serravaliyen–Tortoniyen, ~13.2–8.6 My), Sofular Formasyonu (Burdigaliyen–Langhiyen), Balyatağı Formasyonu (Akitaniyen–Burdigaliyen), Kışlak Formasyonu (Eosen), Okçular Formasyonu (Eosen). Karasu riftinin bulunduğu kesimlereki benzer sedimanlar, Gökdere Formasyonu (Tortoniyen–Messiniyen), Kepez Formasyonu (Langhiyen), Kıcı Formasyonu (Burdigaliyen), ve Hacıdağ Formasyonu (Paleosen–Eosen) olarak isimlendirilmiştir.

Anahtar Sözcükler: Senozoyik stratigrafisi, stronsiyum izotopları, mikropaleontoloji, Hatay Grabeni, Karasu Rifti, Ölü Deniz Fay Zonu

Introduction

The Neogene Hatay Graben and the Karasu Rift are sedimentary basins located in southern Turkey near the border with Syria (Figure 1).

The Hatay Graben is orientated NE–SW and is bounded to the northwest by the Kızıldağ Massif, a range of mountains that extends northwards for ~ 80 km and rises sharply from the Mediterranean Sea and the Gulf of İskenderun to ~1800 m. To the southwest the basin is bounded by Ziyaret Dağ, which rises to ~1300 m. The Hatay Graben, situated between these mountain ranges, descends from 160 m asl (above sea level) in the Amik Plain (northeast of Antakya; Figure 1), inland, down to the coast.

The Karasu Rift, to the northeast, trends northwards from the Amik Plain, with the Kızıldağ/Amanos Dağ to the west (Figure 1) and Syria to the east and south. These basins are situated in a zone of active neotectonics; to the north of the Hatay Graben there is the East Anatolian Fault Zone (EAFZ), to the west the Cyprus Arc and directly to the east is the Dead Sea Fault Zone (DSFZ) that is widely considered to run along the Karasu Rift (Figure 1) (Freund *et al.* 1968; Rojay *et al.* 2001). The Hatay Graben and Karasu Rift are distinctive basins based on their structural style. The Hatay Graben is a transtensional half-graben dominated by normal faults, whereas the Karasu Rift is a strike-slip pull-apart with sinistral boundary faults.

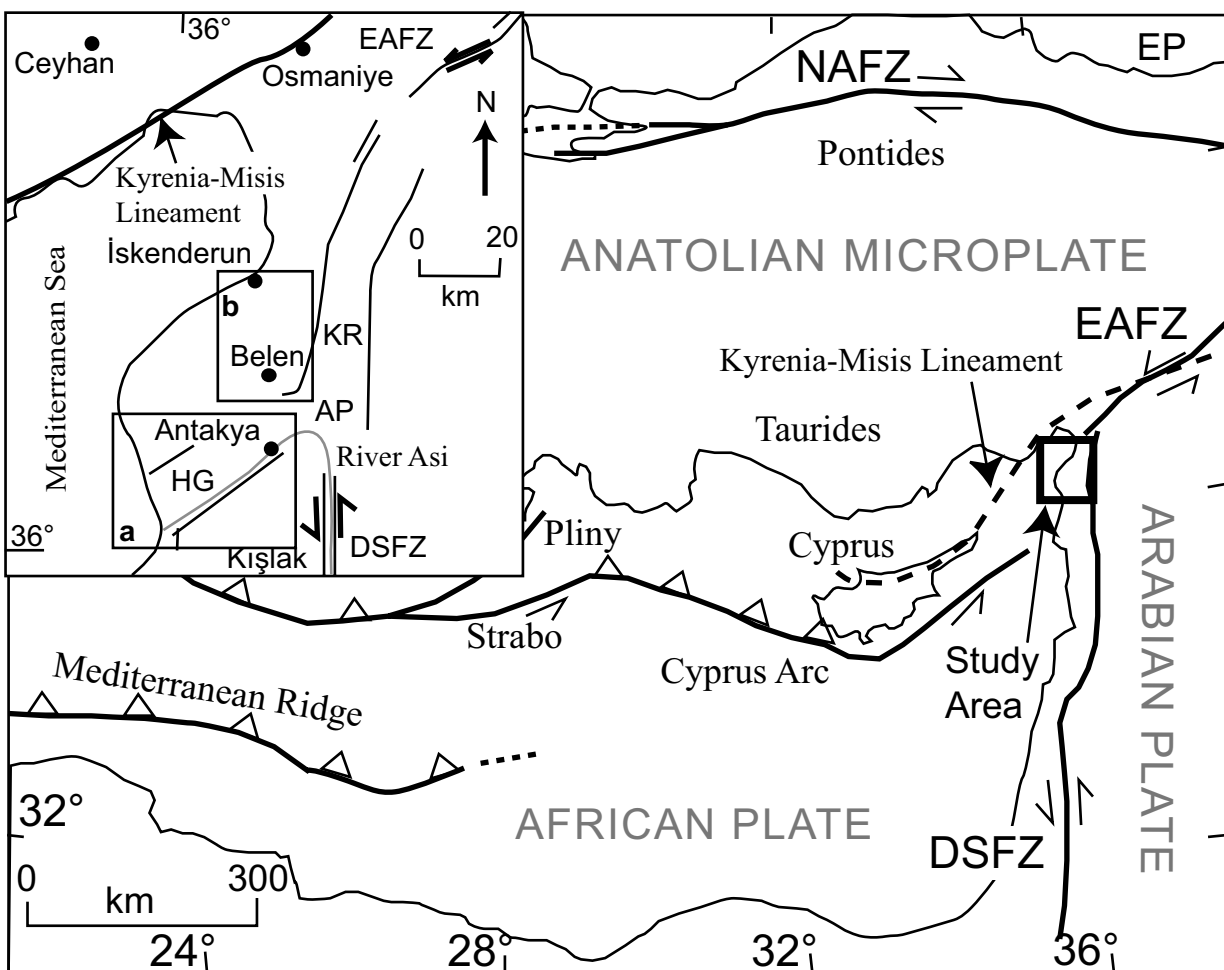


Figure 1. Regional tectonic map of the Eastern Mediterranean; box indicates location of insert. EP– European Plate; DSFZ– Dead Sea Fault Zone; EAFZ– East Anatolian Fault Zone; NAFZ– North Anatolian Fault Zone. Inset box shows in more detail the neotectonic lineaments of the Hatay region. Box a shows the location of Figure 2 and box b, shows the location of Figure 3. HG– Hatay Graben; AP– Amik Plain, KR – Karasu Rift, modified from Boulton *et al.* (2006).

In this paper, we will formally redefine the stratigraphy for the Neogene rocks of the Hatay Graben and the Belen/Kırıkhan area of the Karasu Rift to provide a regionally consistent framework for sedimentological and structural studies. This enables a better understanding of the evolution of the Hatay Graben (e.g., Boulton *et al.* 2006) and facilitates comparisons between these two areas and the wider region. This revision of the stratigraphic nomenclature has been achieved by combining the existing stratigraphy with new field observations, and utilises both published and new micropalaeontological results, and is supported by the first strontium isotope dating of this area.

Previous Stratigraphic Framework

The geology of the Hatay area has attracted much interest due to its location in an area of active neotectonics. The sediments of the Hatay Graben and those exposed around the towns of Kırıkhan and Belen in the Karasu Rift share some lithological similarities and span the same time period (Upper Cretaceous to Recent). Dubertret (1939, 1953) carried out early studies of the area, but a stratigraphy was not available until Atan (1969) divided the Miocene sediments of the entire area into two formations: the Yazır and Enek formations, with the Enek Formation consisting of two members. Atan (1969) also divided Palaeocene to Eocene limestones into two formations, but these were given different names for the areas around Antakya and Kırıkhan (Figures 2–4; Table 1). In the Hatay Graben these formations were named the Okçular and Kışlak formations, whereas in the Karasu Rift sediments of the same age and similar lithology were termed the Cona Formation and the Almacık Limestone. These authors studied the area as a whole, but subsequently the stratigraphy of the two areas was considered separately. Atan's (1969) lithostratigraphic terminology continued to be used in the Hatay Basin (Selçuk 1981; Pişkin *et al.* 1986) until Şafak (1993a) used micropalaeontology to divide the Miocene succession into five new biostratigraphic units; the Balyatağı, Sofular, Tepehan, Nurzeytin and Vakıflı Formations. This terminology was subsequently used by Mistık (2002) and Temizkan (2003) as lithostratigraphic formations. In the northern area a greater variety of nomenclature and divisions gradually came into existence (Table 1) as each successive researcher used their own different terminology, resulting in considerable

confusion. It was, therefore, clear that the lithostratigraphy of the region as a whole needed to be redefined to provide a unified and workable stratigraphy.

Micropalaeontology

Biostratigraphy has been carried out in the area by several authors including Atan (1969), Avşar (1991) and Şafak (1993a, 1993a,b). Planktonic foraminifera and ostracods are plentiful and have been extensively studied. Although benthic foraminifera and coccoliths are present, these have so far not been investigated in this area. Five planktonic foraminiferal biozones can be identified with the Neogene succession of the Hatay Graben (Şafak 1993a; Table 2), and these can be correlated with other areas of the Eastern Mediterranean.

Samples were taken for biostratigraphic dating from measured sections; fourteen sections were sampled but only six sections contained a high enough abundance or suitably well-preserved microfossils for biozone identification. These six sections are labelled with a letter code after their location (Figures 2 & 4): KA– Karalı, KE– Kesecik, OR– Ortatepe, IS– İskender Tepe, SR– Serinyol, PL– Sutası (as another barren sample had been labelled SU already) (Figures 2 & 5–7; Tables 4–7).

In total, 142 ostracod species and 34 planktonic foraminiferal species were identified. Planktic foraminiferal species were identified in all of the sections (Figures 8–10). Ostracods (Figures 11–14) were also identified in most of the sections apart from the İskenderun Tepe (IS) and Serinyol (SR) sections. The microfossil samples successfully dated the sediments of these sections as Middle Miocene, Late Miocene and Pliocene in age and identified the Late Miocene–Pliocene boundary in three of these sections (Tables 4–6). This important boundary had not been recognised at these locations prior to this study.

The Kesecik (KE) section dates from the Middle Miocene and contains the characteristic planktic foraminifera *Orbulina universa* (Figure 8). In the Karalı (KA) section the presence of the planktic foraminifera *Neogloboquadrina acostaensis* (Figure 9), *Neogloboquadrina dutertrei* (Figure 9) and *Pulleniatina finalis* are diagnostic of the Early Pliocene (Table 5). In the Ortatepe section (Table 6) the planktic foraminiferas *Globigerinoides obliquus* (Figure 10) and *Globigerinoides extremus* are diagnostic of the Tortonian and Pliocene.

Table 1. Stratigraphic table showing the various names and definitions of formations as described by various authors.

T e r t i a r y		Antakya (Southern) Area						Kırıkhan (Northern) Area						This Study	
		Atan 1969	Selçuk 1981	Pişkin 1986	Safak 1993	Atan 1969	Derman 1979	Kozlu 1982	Yılmaz 1982	Günay 1984	Kop 1996	South	North		
Pliocene	Neogene	Samandağ	Samandağ	Samandağ	Samandağ						Samandağ				
		Yazır Sofular Mb Enek Balyatağı Mb	Yazır Enek	Yazır Enek	Vakıflı Nurzeytin Tepenan Sofular Balyatağı	Yazır Sofular Mb Enek Balyatağı Mb	Seyhan Karaisalı Gıldırı	Kızıldere Horu Mb Kalecik		Altınözü Teknepinar	Gökdere Kepez Kıcı	Vakıflı Mb Nurzeytin Sofular Balyatağı	Gökdere Kepez Kıcı		
Palaeocene / Eocene	Palaeogene	Kışlak	Kışlak	Kışlak	Kışlak	Almacık Lmst		Kocagedik	Hacıdağı	Hacıdağı	Kışlak	Hacıdağı			
		Okçular	Okçular	Uluylol - Okçular	Okçular	Cona				Cona	Cona	Okçular	Cona		

Table 2. Biostratigraphy compared with formation name and strontium data.

		Formatio		Pla kto ic Forami ifera	Ostracod zo es
Pliocene		Sama dağ			
iocene	essi ia		Vakifi		<i>Cyprideis</i>
	Torto ia				
	Serravallia		N rzeyti	N10 <i>Orbulina universa</i>	<i>Carinocythereis</i>
	La ghia	Sof lar		N9 <i>Orbulina suturalis</i>	
				N8 <i>Praeorbulina glomerosa curva</i>	
B rdigalia	Balyatağı	N7 <i>Globigerinoides trilobus</i>			
Eocene	L tetia	Kışlak Okç lar	P10 <i>Acarinina bullbrooki</i>		

The Pliocene boundary in this section is identified by the appearance of *Globorotalia margaritae*. The ostracod *Urocythereis margaritifera*, in the Sutası (PL) section is the diagnostic fossil of the Early Pliocene. Samples 1–6 in the SR– Serinyol section (Table 8) where sampled from Eocene and Lower Miocene rocks that did not provide fossils; therefore only samples 7–10 should be considered as of Late Miocene age.

Strontium Isotope Stratigraphy

Here, we present the first $^{87}\text{Sr}/^{86}\text{Sr}$ dating of sediments from this area. The pre-existing age determinations were based solely on micropalaeontological studies. Quantitative dating of these sediments, in addition to identifying the age of the sample in question, also allows facies correlations and provides a more complete picture of basin evolution.

$^{87}\text{Sr}/^{86}\text{Sr}$ isotope analysis works on the principle that

the $^{87}\text{Sr}/^{86}\text{Sr}$ isotope ratio of sea-water at any one time is constant throughout the world's oceans due to the fact that the residence time of Sr in sea-water (~2.5–5 Ma) is much greater than the mixing time of the ocean (Broeker & Peng 1982; McArthur 1994). The Sr ratio in sea-water varies due to a number of factors: (a) the amount of high $^{87}\text{Sr}/^{86}\text{Sr}$ terrigenous detrital flux into the ocean from continental weathering relative to the low $^{87}\text{Sr}/^{86}\text{Sr}$ ocean crust input from hydrothermal exchange at mid-ocean ridges; and (b) the dissolution of carbonates on the sea-floor acts as a buffer by adding Sr with a ratio similar to that of sea-water (Brass 1976; McArthur 1994; Oslick *et al.* 1994). The diagenetic carbonate flux is an order of magnitude smaller than the erosion and hydrothermal fluxes.

Much work has been undertaken to constrain the shape of the Sr ratio curve through time (i.e. Miller *et al.* 1991; Hodell & Woodruff 1994; Oslick *et al.* 1994; Gleason *et al.* 2002). This is important because the

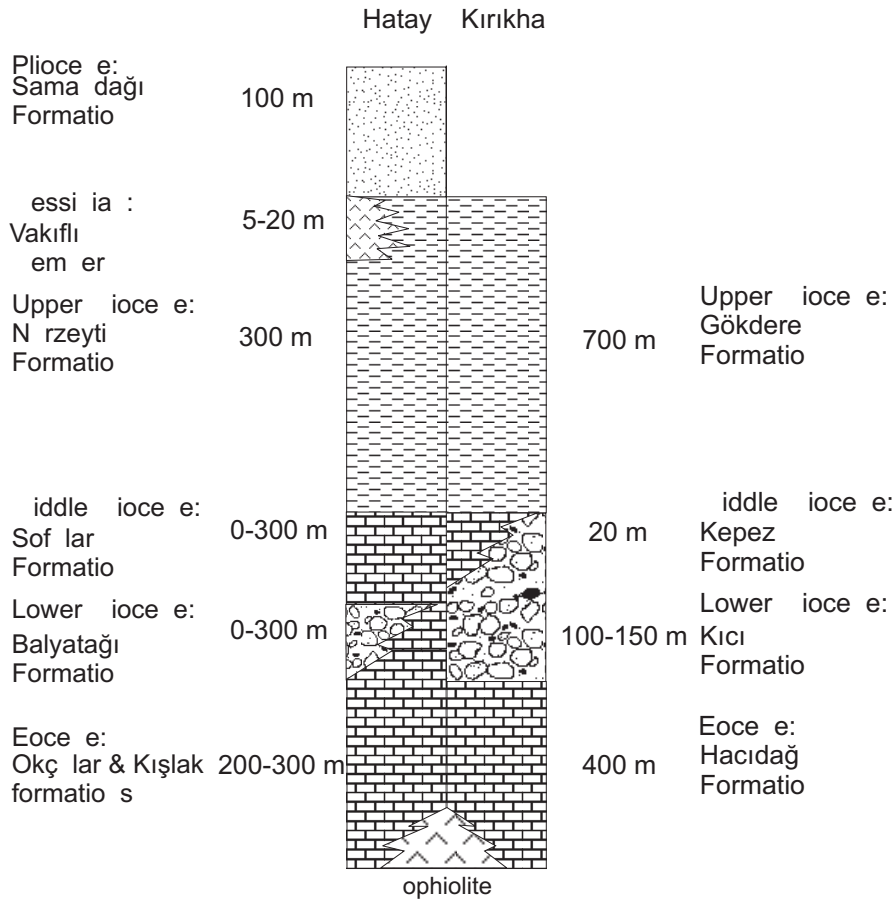


Figure 3. Summary log for the Hatay and Kırıkhan areas showing the formations defined in both areas; not to scale.

highest temporal resolution is obtained for parts of the sea-water curve that have the highest rate of change of $^{87}\text{Sr}/^{86}\text{Sr}$ ratio as a function of time. During the Late Miocene there was a favourable rate of change. However, the method breaks down during the Messinian in the Mediterranean as marginal basins became restricted and the strontium isotope ratio was affected by a change in the ratio of fresh and marine water, and this led to anomalous $^{87}\text{Sr}/^{86}\text{Sr}$ ratios (Flecker *et al.* 2002; Flecker & Ellam 2006).

Strontium is obtained from biogenic carbonate, which is the main sink of Sr in the oceans (Brass 1976; Hodell 1994). Organisms forming carbonate shells or tests do not fractionate Sr isotopes. Thus it can be assumed that the $^{87}\text{Sr}/^{86}\text{Sr}$ ratio in the biogenic carbonate is the same as that of sea-water at the time of precipitation. Radiogenic Sr^{87} from the decay of Rb^{87} can be ignored as biogenic

carbonate generally contains low concentrations of Rb relative to Sr, providing no diagenetic alteration has occurred (Elderfield 1986).

Methodology

Mixed samples of benthic and planktic foraminifera were selected for strontium analysis from the locations (shown on Figures 2 & 15). Bulk rock analysis was excluded as there was a risk of including unknown and reworked components within the sample that could then result in erroneous results. There is also an increased risk of including a diagenetic overprint (Richter & De Paolo 1988). Other marine organisms that construct a calcite shell (e.g., echinoids and oysters) can be used for $^{87}\text{Sr}/^{86}\text{Sr}$ analysis. However, Flecker (1995) has shown that such organisms are generally more affected by diagenesis and have larger error bars than for measurements of

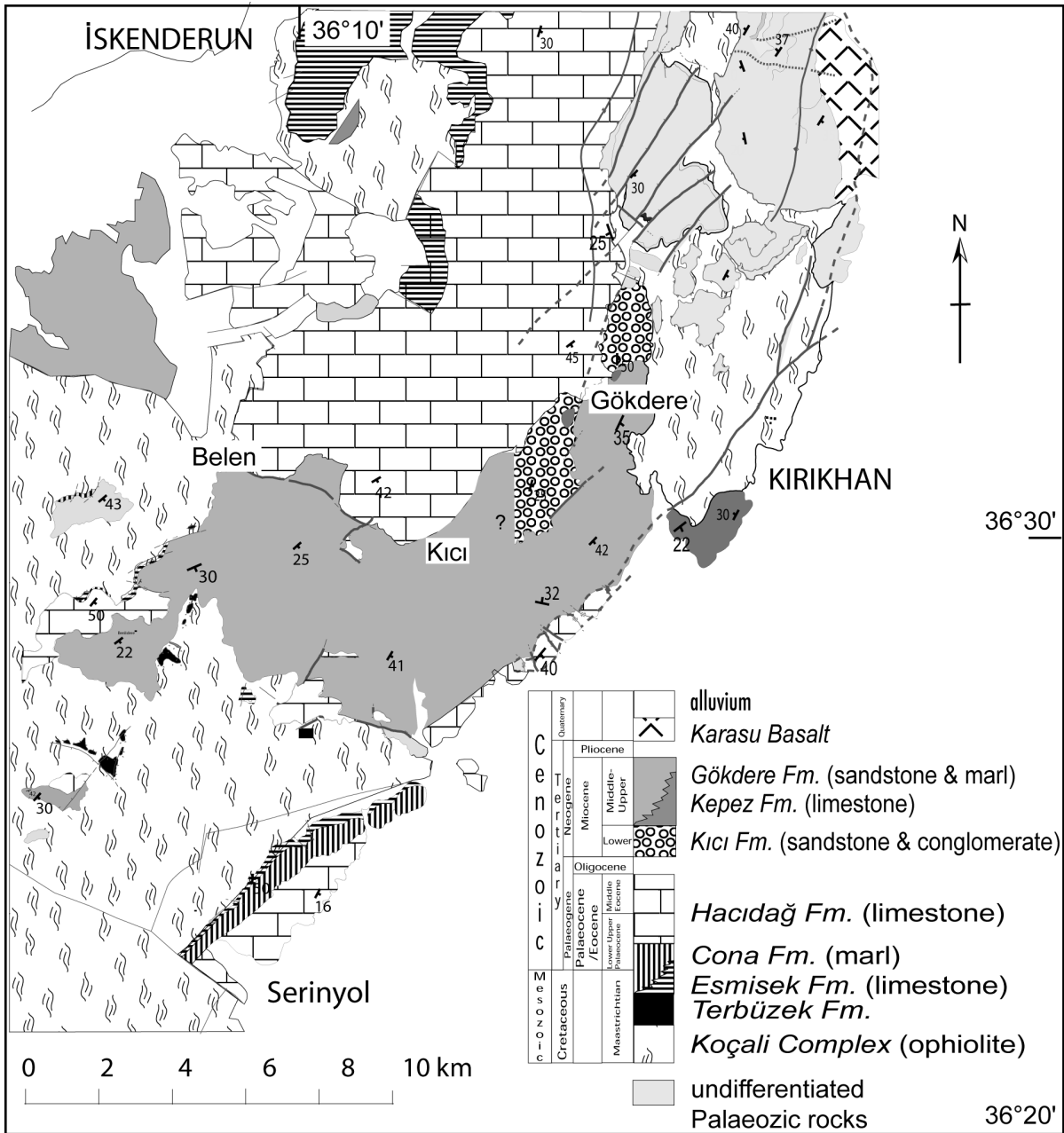


Figure 4. Geological map of area around Belen and Kırıkhan (adapted from Pişkin *et al.* 1986 and Kop 1996) with places discussed in the text indicated. Section SR was measured at Serinyol.

foraminifera alone. For this reason it was decided to use only foraminifera for $^{87}\text{Sr}/^{86}\text{Sr}$ ratio determination. Samples of mixed benthic and planktic species were used, as there is no evidence in the literature to show that fractionation between the forms can occur.

Foraminifera were processed to extract the strontium from the test. Ammonium acetate was first added to the

samples in order to leach and remove any remaining clay minerals and strontium adhering to the foraminifer tests after cleaning. The strontium was then extracted by dissolving the samples and loading the resulting solution into cation exchange columns. The processed samples were loaded onto Ta filaments in the standard manner and placed within a 20-sample turret. The isotope ratios















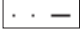







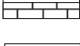





KEY			
	fossiliferous marl, thickness >20 cm		oolite
	fossiliferous marl, thickness <20 cm		bivalve
	fossiliferous marl		whole echinoid
	calcarenite		gastropod
	arenite		parallel lamination
	interbedded arenite and marl, bed thickness 0.01-0.3 m		ripple marks
	mudstone with thin sandstone interbeds <15 cm		slump
	silt		horizontal rows
	marl		vertical rows
	conglomerate		cross-bedding
	ophiolite (serpentine)		plant material
	interbedded micritic and marl, bed thickness 0.1-0.3 m		coral
	gypsum		Foraminifera
			ripples
			Oyster

Figure 5. Key for symbols used in the sedimentary logs.

were measured on a VG Sector 54-30 mass spectrometer in dynamic multicollection mode with mass fractionation normalized to a $\text{Sr}^{86}/\text{Sr}^{88}$ ratio of 0.1194. The mean of NIST SRM987 since March '04 is 0.710254 ± 20 (2 S.D., $n=45$). The results obtained are set out in Table 3.

Results (Table 3; Figure 16)

The ages (Table 3; Figure 9) were calculated (using an excel spreadsheet) from the measured $^{87}\text{Sr}/^{86}\text{Sr}$ ratios using the seawater curves of Howarth & McArthur (1997) and McArthur *et al.* (2001). Some samples were chosen in order to date sediments of unknown age. Samples SB39A and SB44 yield Late Miocene ages. However, SB39A yielded an average age of 13.24 Ma, older than anticipated from the field relationships, which indicate that the sample came from near the upper

boundary of the Upper Miocene sediments. SB47A is Pliocene in age. Surprisingly, sample SB67 gave a Messinian age (average age – 5.35 Ma). This sample is from a location near to the basin margin in the northwest, in what was considered to be marl of Late Miocene age, based on sedimentary facies and lateral correlations. A high Rb content in the sample has probably resulted in an anomalous result, which would not be reliable in any case as Sr dating is not applicable to the Messinian of the Mediterranean, as noted above.

Samples SB18A, SB20A and SB22A were collected sequentially up-sequence from an Upper Miocene section near the village of Mızraklı. A pre-Messinian age was expected as this section stratigraphically underlies gypsum. Samples SB18A–20A show an upward decrease in age over ~16 m, as expected, from 9.05 Ma to 8.68 Ma, indicating a Tortonian age for these marls. However,

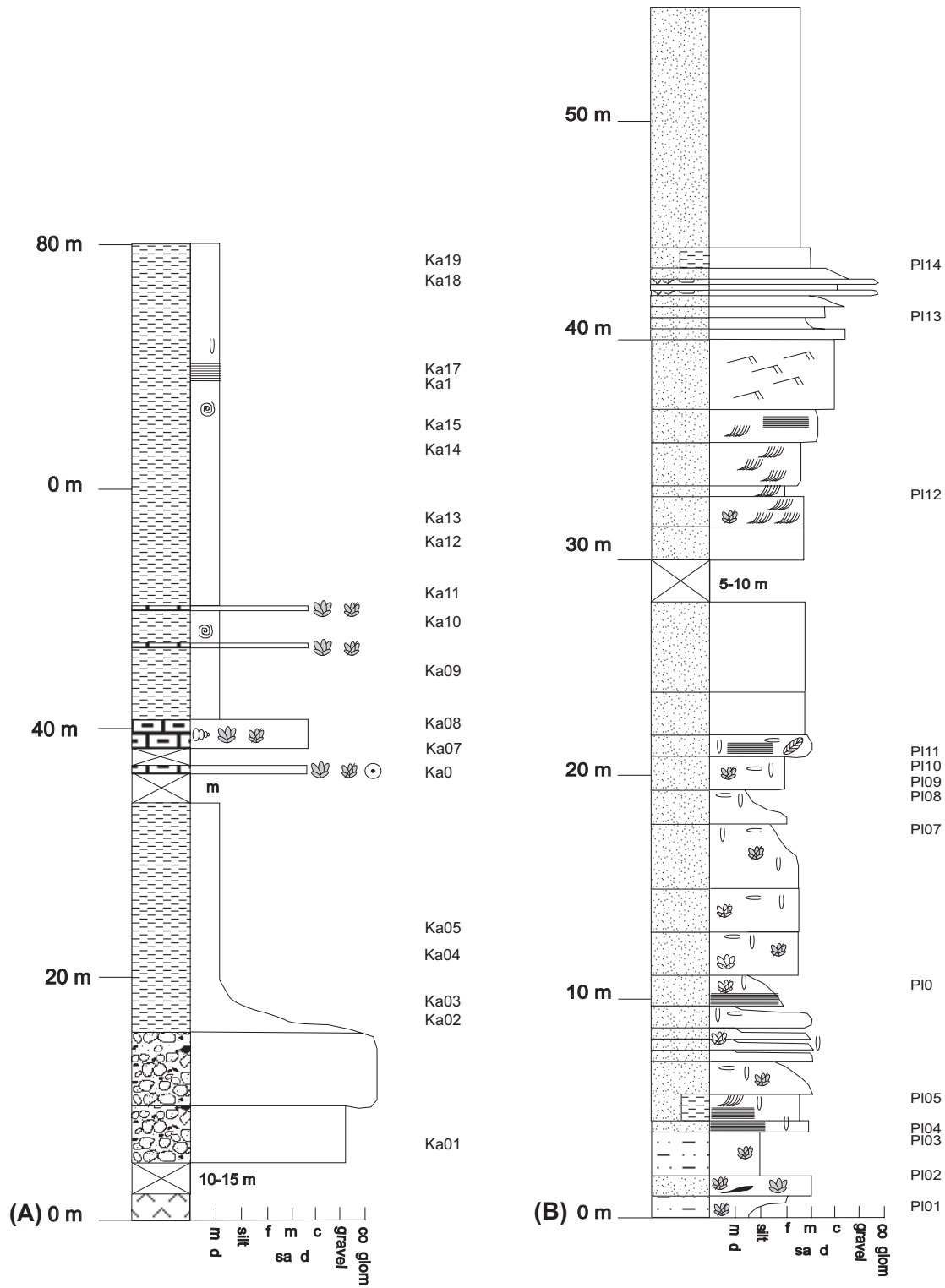


Figure 6. (A) Log of the Karalı section showing the sedimentology and stratigraphic positions of samples used for micropalaeontology (Table 5); (B) Log of the Sutası section showing the stratigraphic position of samples used for micropalaeontology (Table 7), NB: Sample numbers were given a PL label as the SU label had already been used.

Table 3. New strontium isotope results for the Hatay Graben.

Sample	$^{87}\text{Sr}/^{86}\text{Sr}$	2SE	Age (Ma)	Range	Range (inc 2SE)	Stage
SB18A	0.708919	21	9.05	8.82–9.28	7.42–10.04	Tortonian
SB20A	0.708925	18	8.68	8.41–8.93	7.17–9.79	Tortonian
SB22A	0.708878	23	10.84	10.53–10.74	9.87–11.33	Tortonian
SB39A	0.708812	23	13.24	13.08–13.39	12.09–14.57	Serravalian
SB44	0.70893	21	8.33	8.03–8.60	6.93–9.68	Tortonian
SB42A	0.708894	21	10.06	9.93–10.19	9.04–10.91	Tortonian
SB47A	0.709023	23	5.35	5.20–5.41	4.59–5.80	Mio/Plio
SB50A	0.70891	18	9.46	9.39–9.81	8.03–10.34	Tortonian
SB56A	0.708907	21	9.58	9.42–9.72	7.53–10.48	Tortonian
SB67	0.709009	23	5.61	5.56–5.66	5.01–6.06	Messinian
SB80	0.708861	21	11.22	11.11–11.33	10.39–12.13	Tortonian
SB81	0.708924	21	8.75	8.48–8.99	7.17–9.86	Tortonian

sample SB22A, ~10 m higher in the sequence yielded, a much older age than expected, i.e. 10.84 Ma, well outside the range of analytical error. If this sample had come from the upper part of the section this anomalous result could reflect basin isolation (i.e. pre-salinity crisis) leading to reduced $\text{Sr}^{87}/\text{Sr}^{86}$ values and thus an erroneous age value. However, as the sample is near the base of the sequence this seems unlikely (although not impossible). Alternative explanations of the unexpected result are that the analysed foraminifera are reworked (and so older), or that diagenesis has affected the Sr isotopic ratios. The sample did, indeed, come from a stratigraphic horizon that contains small iron nodules of diagenetic origin. Another alternative is that the formation is faulted, but this was not observed in the field.

Samples SB18A, SB50 and SB42A were taken from the Middle–Upper Miocene boundary (Sofular/Nurzeytin formations) in order to investigate the age of this contact. SB18A was taken from the base of the Mızraklı section in the southwest of the basin; as noted above this sample yielded an average age of 9.05 Ma. Sample SB50 was taken from the boundary section exposed in the Karaçay valley; this sample yielded an average age of 9.46 Ma. Sample SB42A was collected to the northwest of SB50 at location 180. At this location, thick bioclastic limestone

with interbedded marl and marly limestones are exposed in the hanging wall of a normal fault. This lithology is similar to the Middle to Upper Miocene boundary limestone. Sample SB42A was taken from the first marl interval above this hard limestone. The footwall of the fault is composed of hard bioclastic limestone. This sample yielded an average age of 10.06 Ma. Sample SB56A was collected near the Middle to Upper Miocene boundary even further to north and this sample gave an average age of 9.58 Ma.

Taking the average ages and assuming that these samples come from the same lithostratigraphic boundary interval this appears to indicate that the boundary in the northeast of the basin (i.e. inland today) is generally older than the equivalent boundary to the southwest (i.e. towards the present coast). Another factor to take into account is the planktic and benthic foraminiferal ratio, which is indicative of water depth, assuming the material is not redeposited or reworked. Samples SB50 and SB56A have a planktic: benthic ratio (P/P+B) of 0.59, whereas SB18A has a ratio of 1 and SB42A has a ratio of 0.08. This suggests that SB18A accumulated in shallow-water, whereas SB42A is fully marine origin (~200 m) and the other samples were deposited at intermediate water depths.

Table 4. Distribution of planktonic foraminifera and ostracods from the section at Kesecik village. The section was measured from 0238982/4015161, topographic map Antakya P36-d1.

T e r t i a r y				SYSTEM KE - KESECİK VILLAGE
N e o g e n e				
M i o c e n e		M i d d l e		SERIES
Sofular Formation				FORMATION
→	↺	↻	↵	SAMPLE NUMBER
				OSTRACODA
				Planktonic Foraminifers
		+	+	<i>Cytherella vulgata</i> Ruggieri
		+		<i>Bairdia subdeltoidea</i> (Muenster)
+				<i>Cnestocythere truncata</i> (Reuss)
+				<i>Krithe monosteracensis</i> (Sequenza)
+				<i>Acanthocythereis hystrix</i> (Reuss)
	+			<i>Costa edwardsii</i> (Roemer)
+	+			<i>Chrysocythere paradisus</i> Doruk
	+			<i>Cistacythereis pokorny</i> (Ruggieri)
+				<i>Keijella hodgii</i> (Brady)
+		+		<i>Ruggieria tetraptera</i> (Sequenza)
+				<i>Procythereis sulcatopunctatus</i> (Reuss)
+				<i>Echinocythereis scabra</i> (Muenster)
+				<i>Aurila convexa</i> (Baird)
+				<i>Aurila albicans</i> (Ruggieri)
+				<i>Aurila</i> sp. B Bassiouni
+				<i>Pokornyella deformis minor</i> (Moyes)
+	+			<i>Hermanites haidingeri minor</i> Ruggieri
+				<i>Xestoleberis ventricosa</i> Müller
+				<i>Xestoleberis communis</i> Müller
		+	+	<i>Globigerinoides trilobus</i> (Reuss)
	+		+	<i>Globigerinoides sacculifer</i> (Brady)
+				<i>Globigerinoides immaturus</i> Le Roy
			+	<i>Globigerinoides ruber</i> (d'Orbigny)
			+	<i>Globoquadrina dehiscens</i> (Chapman, Parr & Collins)
		+	+	<i>Praeorbulina glomerosa curva</i> (Blow)
		+	+	<i>Orbulina bilobata</i> (d'Orbigny)
+	+	+	+	<i>Orbulina suturalis</i> Brönnimann
+			+	<i>Orbulina universa</i> d'Orbigny
		+		<i>Globigerinella obesa</i> (Bolli)

Table 5. Distribution of planktonic foraminifera and ostracods from the section at Karali village, section measured from 0243641/4019688, topographic map Antakya P36-a3.

Tertiary		SYSTEM	KA- Karali																			
Neogene																						
Middle - Late Miocene		SERIES	FORMATION																			
Nurzeytin Formation																						
Early Pliocene		SAMPLER NUMBER																				
Samandağ Fm.																						
1	2	3	4	5	6	7	8	9	10	11	12	13	14	15	16	17	18	19	20	21		
OSTRACODA																					Planktonic Foraminifers	
																					<i>Cytherelloidea glypta</i> Doruk	
																					<i>Bairdia subdeltoidea</i> (Muenster)	
																					<i>Neonesidea corpulenta</i> (Müller)	
																					<i>Cyprideis torosa</i> (Jones)	
																					<i>Krithe monosteracensis</i> (Sequenza)	
																					<i>Acanthocythereis hystrix</i> (Reuss)	
																					<i>Costa edwardsii</i> (Roemer)	
																					<i>Costa batei</i> (Brady)	
																					<i>Incongruella rotundata</i> (Ruggieri)	
																					<i>Keijella hodgii</i> (Brady)	
																					<i>Procythereis sulcatopunctatus</i> (Reuss)	
																					<i>Aurila convexa</i> (Baird)	
																					<i>Aurila speyeri</i> (Brady)	
																					<i>Aurila freudenthali</i> Sissingh	
																					<i>Aurila</i> sp. B Bassiouni	
																					<i>Aurila soummamensis</i> Coutelle & Yassini	
																					<i>Pokornyella deformis minor</i> (Moyes)	
																					<i>Hermanites haidinger minor</i> Ruggieri	
																					<i>Tenedocythere mediterranea</i> Ruggieri	
																					<i>Tenedocythere prava</i> (Baird)	
																					<i>Loxocorniculum quadricornis</i> (Ruggieri)	
																					<i>Xestoleberis ventricosa</i> Müller	
																					<i>Xestoleberis communis</i> Müller	
																					<i>Xestoleberis glabrescens</i> (Reuss)	
																					<i>Globigerinoides trilobus</i> (Reuss)	
																					<i>Globigerinoides sacculifer</i> (Brady)	
																					<i>Globigerinoides obliquus</i> Bolli	
																					<i>Globigerinoides extremus</i> Bolli & Bermudez	
																					<i>Globigerinoides bisphericus</i> Todd	
																					<i>Globigerinoides ruber</i> (d'Orbigny)	
																					<i>Globigerinoides subquadratus</i> Brönnimann	
																					<i>Praeorbulina glomerata curva</i> (Blow)	
																					<i>Praeorbulina glomerata glomerata</i> Blow	
																					<i>Orbulina suturalis</i> Brönnimann	
																					<i>Orbulina universa</i> d'Orbigny	
																					<i>Orbulina bilobata</i> (d'Orbigny)	
																					<i>Globigerinella obesa</i> (Bolli)	
																					<i>Paragloborotalia mayeri</i> Cushman & Ellisor	
																					<i>Neogloboquadrina acostaensis</i> (Blow)	
																					<i>Neogloboquadrina dutertrei</i> (d'Orbigny)	
																					<i>Globoquadrina venezuelana</i> Hedberg	
																					<i>Globigerina ouachitaensis</i> Howe & Wallece	
																					<i>Globoturborotalita euapertura</i> Jenkins	
																					<i>Pulleniatina finalis</i> Banner & Blow	
																					<i>Dentoglobigerina altispira altispira</i> <small>Cushman & Jarvis</small>	

O: reworked

Table 6. Distribution of planktonic foraminifera and ostracods from the section at Ortatepe, section measured from 0230398/3999093, topographic map Antakya P36-d4.

Tertiary															SYSTEM	
Neogene																
Late Miocene					Early Pliocene										SERIES	
Samandağ Formation															FORMATION	
1	2	3	4	5	6	7	8	9	10	11	12	13	14	15	SAMPLE NUMBER	
															OSTRACODA	
															Planktonic Foraminifers	
															+	<i>Cyprideis anatolica</i> Bassiouni
																<i>Cyprideis torosa</i> (Jones)
																<i>Pontocythere elongata</i> (Brady)
															+	<i>Ruggieria tetraptera</i> (Sequenza)
																<i>Heterocythereis albomaculata</i> (Baird)
																<i>Aurila speyeri</i> (Brady)
																<i>Aurila</i> sp. (B) Bassiouni
																<i>Aurila convexa</i> (Baird)
																<i>Urocythereis favosa</i> (Roemer)
															+	<i>Loxoconcha turbida</i> Müller
															+	<i>Loxoconcha tumida</i> Brady
															+	<i>Loxoconcha alata</i> Brady
																<i>Xestoleberis plana</i> Müller
																<i>Globigerinoides ruber</i> (d'Orbigny)
																<i>Globigerinoides obliquus</i> Bolli
																<i>Globigerinoides extremus</i> Bolli & Bermudez
																<i>Globigerinoides sacculifer</i> (Brady)
																<i>Globigerinella obesa</i> (Bolli)
																<i>Globorotalia margaritae</i> Bolli & Bermudez

The planktic to benthic ratios suggest that the samples come from different locations on the shelf, for which SB42A is the deepest and SB18A is the shallowest. Assuming the sediments simply overlapped a slope, one would expect SB42A to be the youngest and SB18A the oldest. However, when the range of ages determined is taken into account, all lie within a similar time range. This then suggests that the boundary is of the same age across the whole area, and that samples were taken from various depths along a carbonate ramp that underwent synchronous onlap.

Samples SB80 and SB81 were collected from the footwall and the hanging wall of an inferred fault. Although not exposed, the presence of a fault was

inferred from topographic and lithological information in the field. SB80 is dated at ~11.22 Ma, whereas SB81 is dated at ~8.75 Ma. The two sample sites are separated by only ~200 m laterally, in an area where the bedding dips at only 10°. Such a large age difference (~ 2.5 Ma) is unlikely assuming only normal sedimentary processes but is consistent with the presence of a structural break, probably a normal fault dipping to the west.

New Lithostratigraphy of the Hatay Region

The results of the new micropalaeontological study and the strontium dating have been combined with existing micropalaeontological results and new field observations

Table 7. Distribution of planktonic foraminifera and ostracods from the section at Sutaşı village, section measured from 0230000/3997800, topographic map Antakya P36-d4.

T e r t i a r y														SYSTEM
N e o g e n e														
Late Miocene							Early Pliocene							SERIES
Samandağ Formation														FORMATION
1	2	3	4	5	6	7	8	9	10	11	12	13	14	SAMPLE NUMBER
														OSTRACODA
							+							Planktonic Foraminifers
									+	+				<i>Cyprideis torosa</i> (Jones)
			+						+	+				<i>Cyprideis anatolica</i> Bassiouni
											+			<i>Miocyprideis goekcena</i> Bassiouni
									+					<i>Miocyprideis sarmatica</i> (Zalanyi)
										+			+	<i>Cytheridea acuminata acuminata</i> Bosquet
													+	<i>Ruggieria tetraptera</i> (Sequenza)
			+	+					+					<i>Heterocythereis albomaculata</i> (Baird)
			+	+					+	+				<i>Aurila skalae</i> Uliczny
			+						+	+				<i>Aurila convexa</i> (Baird)
			+											<i>Aurila speyeri</i> (Brady)
													+	<i>Urocythereis favosa</i> (Roemer)
											+			<i>Urocythereis margaritifera</i> (Müller)
													+	<i>Cytheretta semiornata</i> (Egger)
													+	<i>Hirschmannia viridis</i> (Müller)
													+	<i>Xestoleberis reymenti</i> Ruggieri
													+	<i>Xestoleberis communis</i> Müller
													+	<i>Xestoleberis plana</i> Müller
													+	<i>Candona (C) parallela pannonica</i> Zalanyi

concerning the sedimentology of the formations to form the basis of the revised stratigraphic framework for the area as set out below. This follows the procedures of the International Commission on Stratigraphy (Hedberg 1976; Murphy & Salvador 1999). The basis of this stratigraphy is that all formations must be mappable units. Where possible, existing stratigraphical units have been refined and formalised, avoiding the introduction of new names. For each stratigraphical unit below, we explain the previous nomenclature (synonymy), give the formation, or member name and its type location, and summarise its lithology and facies variation. In addition, the lower and upper boundaries of each stratigraphical unit are defined and also their thickness and lateral extent. Lastly, the age evidence is summarised, both pre-

existing and resulting from this work. A brief interpretation of the revised stratigraphy as a whole is given following this.

Lithostratigraphic Units of the Hatay Graben

Okçular Formation: Fine-grained Wackestones

Synonymy: Uluyol-Okçular Formation, Pişkin *et al.* (1986).

Name and Type Location: The formation is named after Yukarıokçular village, 12 km south of Antakya (Figure 2).

Lithology and Variation (Figure 17): The Okçular Formation is composed of creamy white limestones,

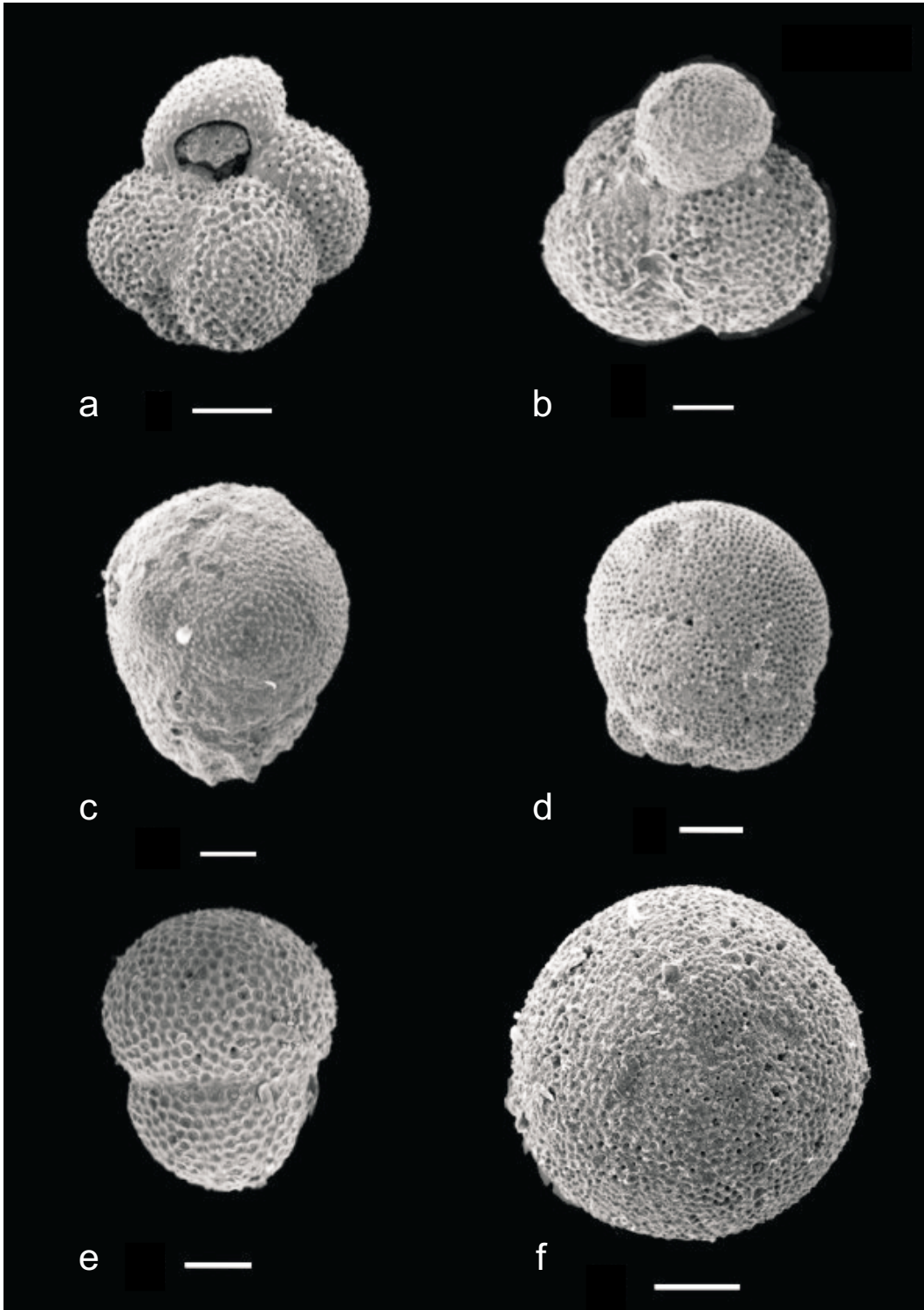


Figure 8. (a) *Globigerinoides extremus* (Bolli & Bermudez), measured section at Karali, Sample 21; umbilical view; scale bar 100 µm; (b) *Globigerinoides ruber* (d'Orbigny), measured section at Karali, Sample 21; spiral view; scale bar 100 µm; (c) *Praeorbulina glomerosa curva* (Blow); measured section at Karali; Sample 16; scale bar 100 µm; (d) *Orbulina bilobata* (d'Orbigny), measured section at Kesecik; Sample 4; scale bar 100 µm; (e) *Orbulina suturalis* Brönnimann, measured section at Kesecik; Sample 4; scale bar 100 µm; (f) *Orbulina universa* d'Orbigny, measured Section at Karali; Sample 16; scale bar 100 µm.

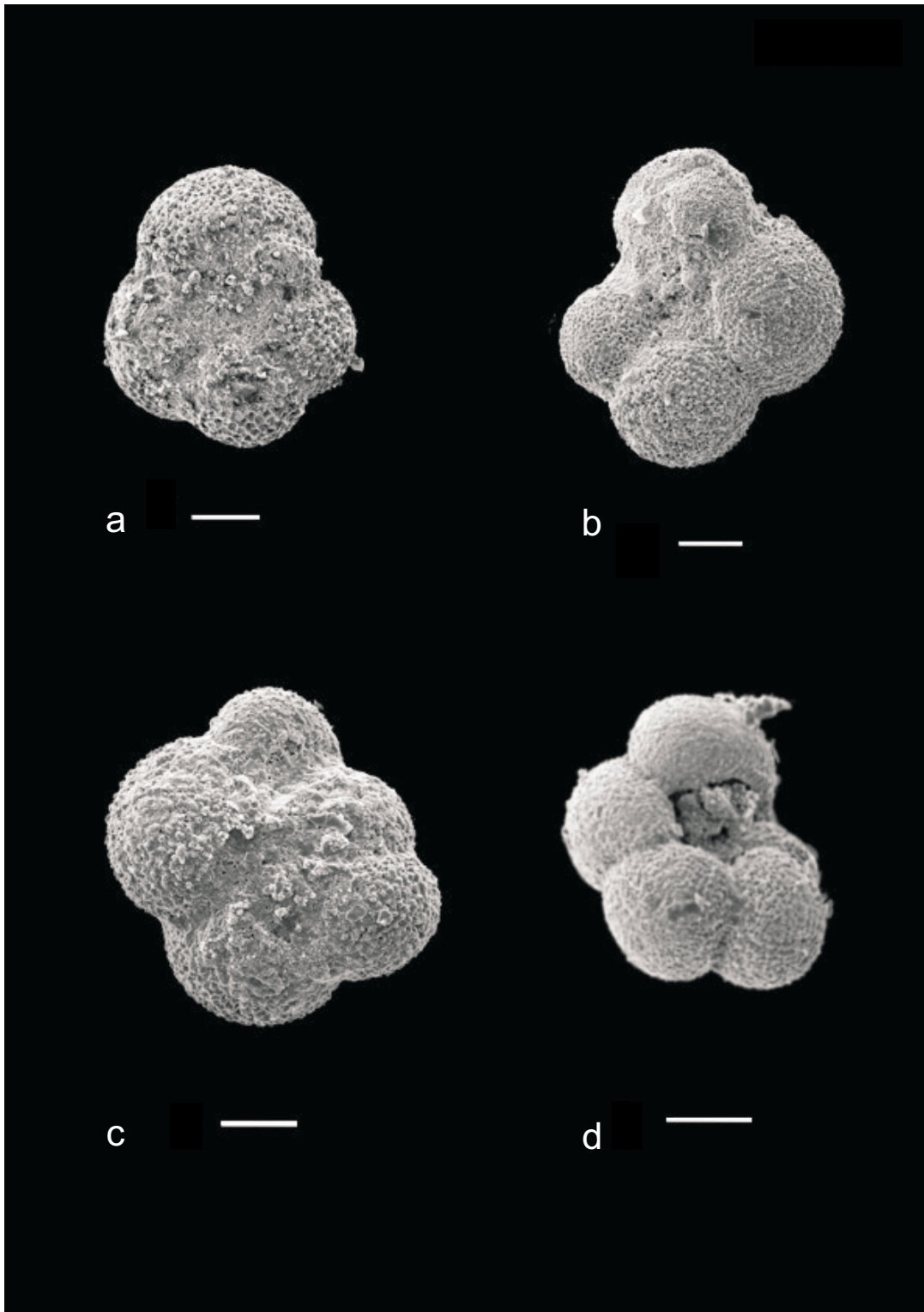


Figure 9. (a) *Paraglobobulimina mayeri* (Cushman & Ellis), measured section at Karali; Sample 18; scale bar 100 µm; (b-c) *Neogloboquadrina dutertrei* (d'Orbigny); measured section at Karali; Sample 18; (b) umbilical view, (c) spiral view; scale bar 100 µm; (d) *Neogloboquadrina acostaensis* (Blow); measured section at Karali; Sample 16; umbilical view; scale bar 100 µm.

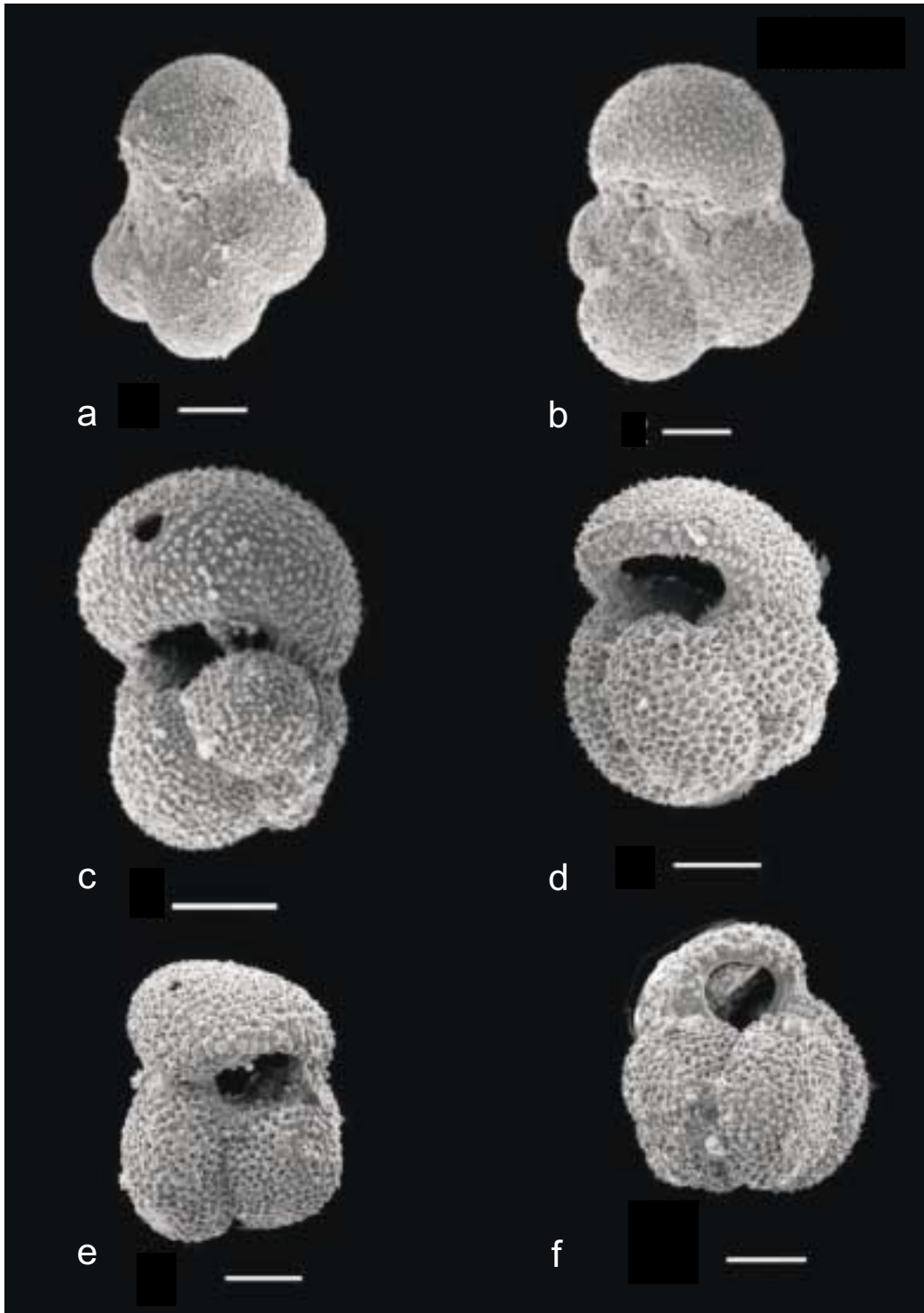


Figure 10. (a) *Globigerinella obesa* (Bolli), measured section at Karali; Sample 16; spiral view; scale bar 100 µm; (b) *Globigerinella praesiphonifera* (Blow); measured section at Kesecik; Sample 4; umbilical view; scale bar 100 µm; (c) *Globigerinoides trilobus* (Reuss); measured section at Serinyol; Sample 8; lateral view; scale bar 100 µm; (d–f) *Globigerinoides obliquus* (Bolli); (d) Umbilical view, measured section at Karali; Sample 19; (e) Lateral view, measured section at Ortatepe; Sample 10; (f) Umbilical view, measured section at Karali, Sample 21, all scale bars 100 µm.

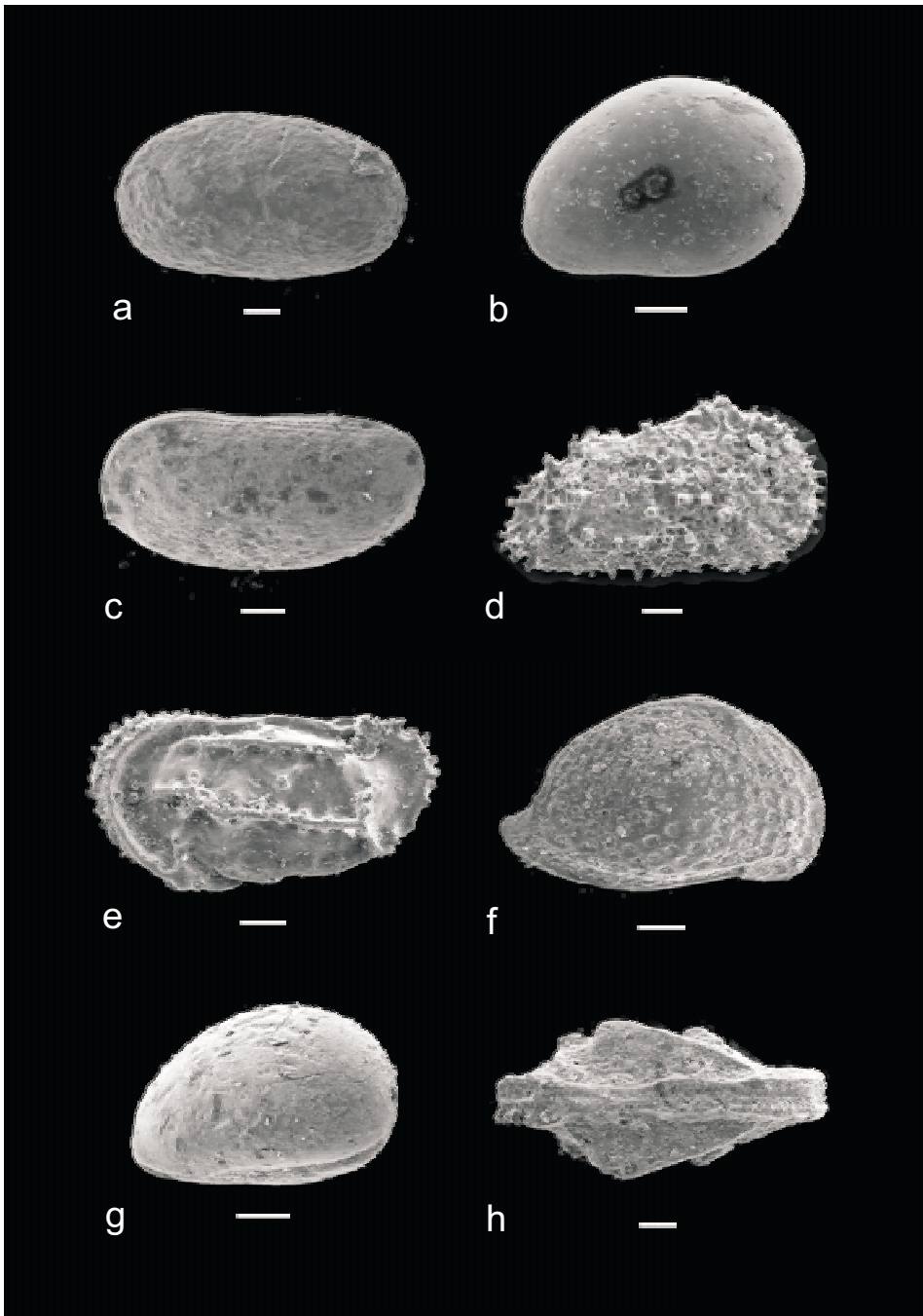


Figure 11. (a) *Cytherelloidea glypta* (Doruk), measured section at Karali; Sample 6; right valve, outside view; scale bar 100 μm ; (b) *Neonesidea corpulenta* (Müller); measured section at Karali; Sample 9; carapace, left side view; scale bar 100 μm ; (c) *Cyprideis torosa* (Jones), measured section at Ortatepe; Sample 5; carapace, right side view; scale bar 100 μm ; (d) *Miocyprideis sarmatica* (Zalanyi), measured section at Sutasi; Sample 8; carapace, left side view; scale bar 100 μm ; (e) *Cyprideis anatolica* Bassiouni, measured section at Sutasi; Sample 10; carapace, left side view; scale bar 100 μm ; (f) *Krithe monosteracensis* (Sequenza), measured section at Karali; Sample 9; carapace, right side view; scale bar 100 μm ; (g) *Acanthocythereis hystrix* (Reuss), measured section at Karali; Sample 21; right valve, outside view; scale bar 100 μm ; (h) *Costa batei* (Brady), measured section at Karali; Sample 21; right valve, outside view; scale bar 100 μm .

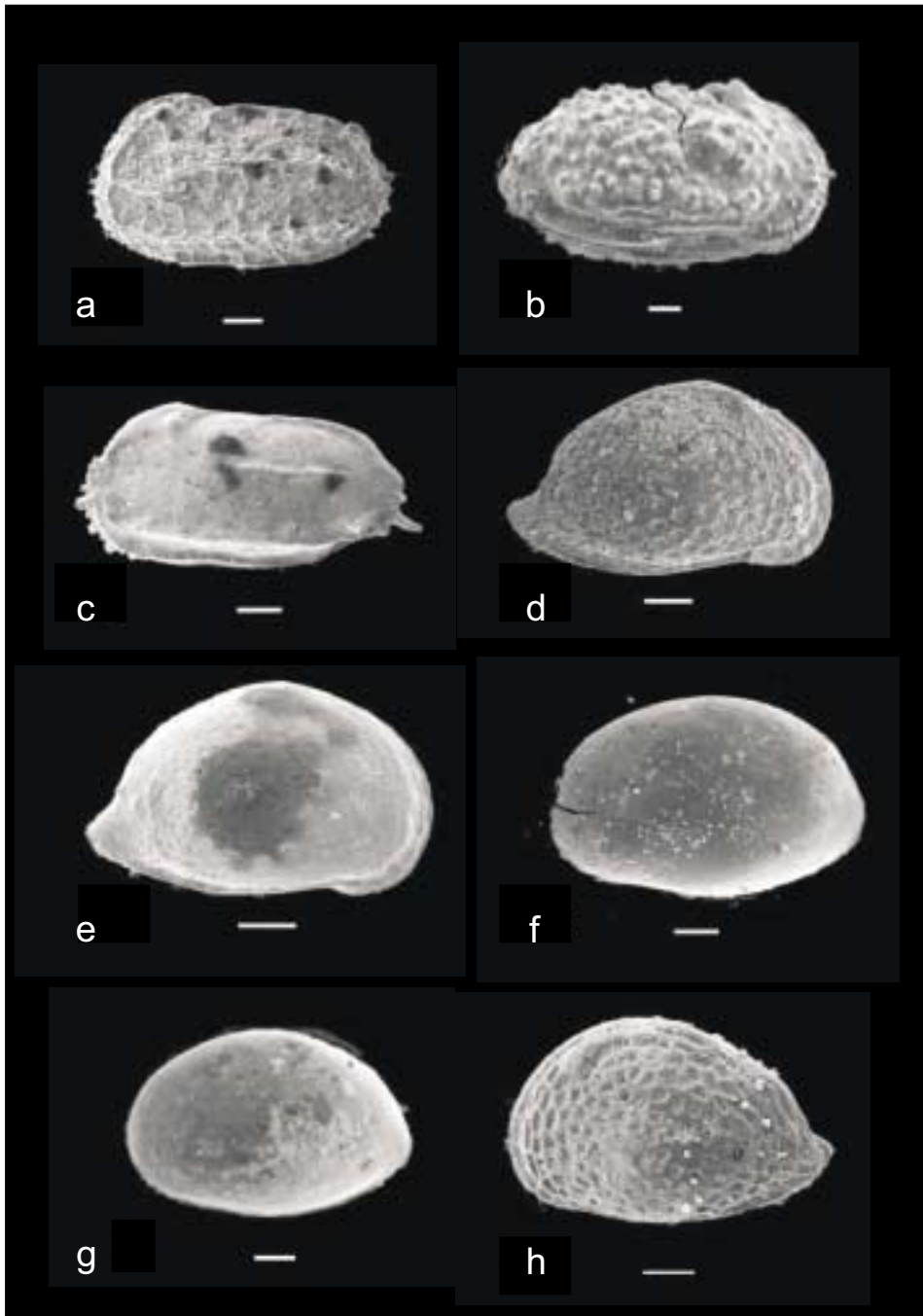


Figure 12. (a) *Chrysocythere paradisis* (Doruk), measured section at Kesecik; Sample 1; right valve, outside view; scale bar 100 μm ; (b) *Echinocythereis scabra* (Münster), measured section at Kesecik; Sample 1; carapace, right side view; scale bar 100 μm ; (c) *Ruggieria tetraptera tetraptera* (Sequenza), measured section at Ortatepe; Sample 5; left valve, outside view; scale bar 100 μm ; (d) *Aurila convexa* (Baird), measured section at Kesecik; Sample 1; right valve, outside view; scale bar 100 μm ; (e) *Aurila albicans* (Ruggieri), measured section at Kesecik; Sample 1; right valve, outside view; scale bar 100 μm ; (f–g) *Aurila skaliae* Uliczny, (f) left valve outside view; measured section at Sutaşı; Sample 2, (g) left valve, outside view; measured section at Sutaşı; Sample 8; scale bar 100 μm ; (h) *Aurila* sp. B Bassiouni, measured section at Kesecik; Sample 1; left valve, outside view; scale bar 100 μm .

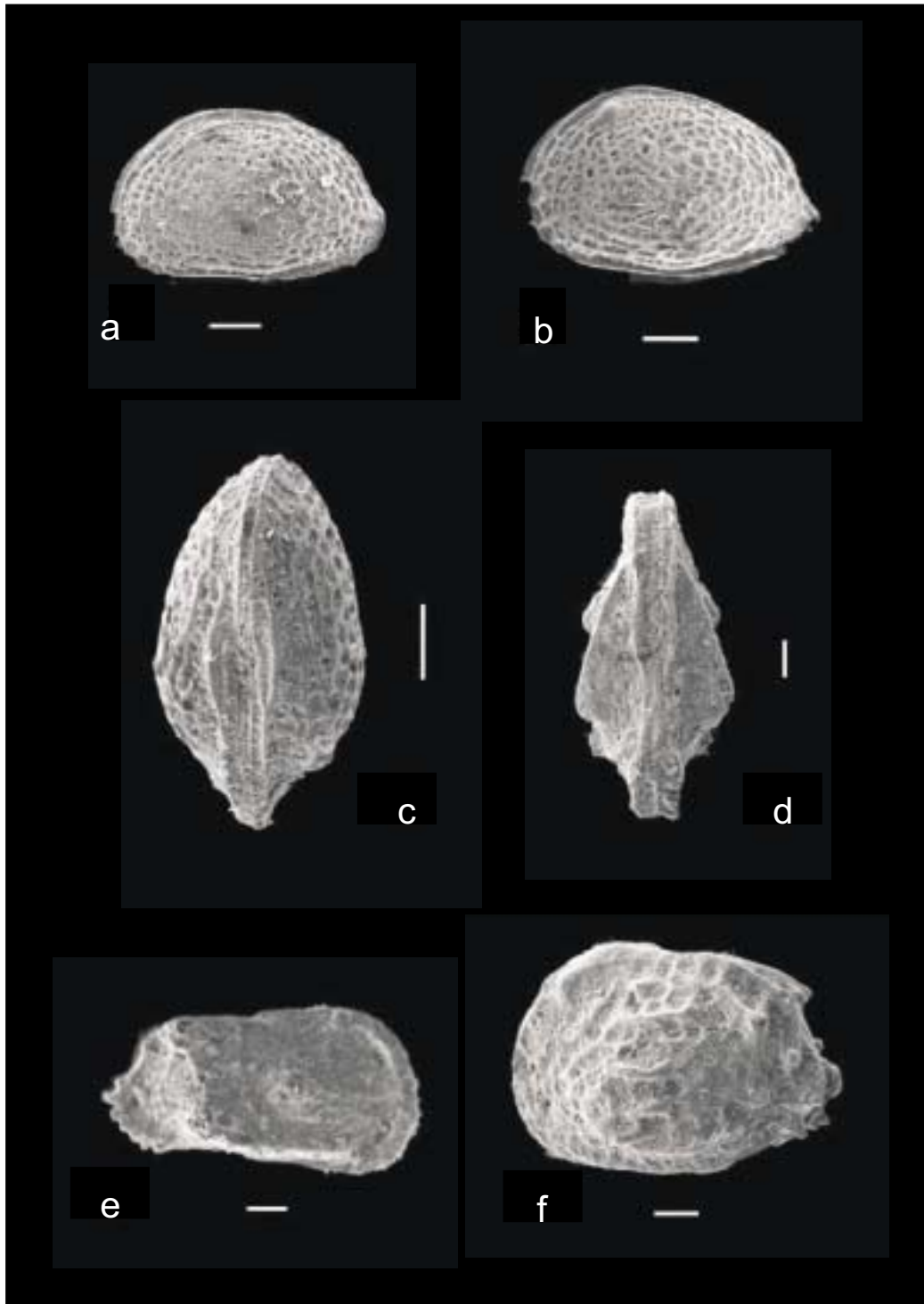


Figure 13. (a) *Pokornyella deformis minor* (Moyes), measured section at Kesecik, Sample 1, carapace, left side view, scale bar 100 µm; (b-c) *Pokornyella deformis minor* (Moyes), measured section at Kesecik, Sample 2, (b) carapace, left side view, (c) carapace, dorsal side view, scale bar 100 µm; (e-f) *Hermanites haidingeri minor* Ruggieri, measured section at Kesecik, Sample 1, (e) carapace, dorsal side view (f) carapace, right side view, scale bar 100 µm; (g) *Tenedocythere prava* (Baird), measured section at Karali, Sample 10, carapace, left side view, scale bar 100 µm.

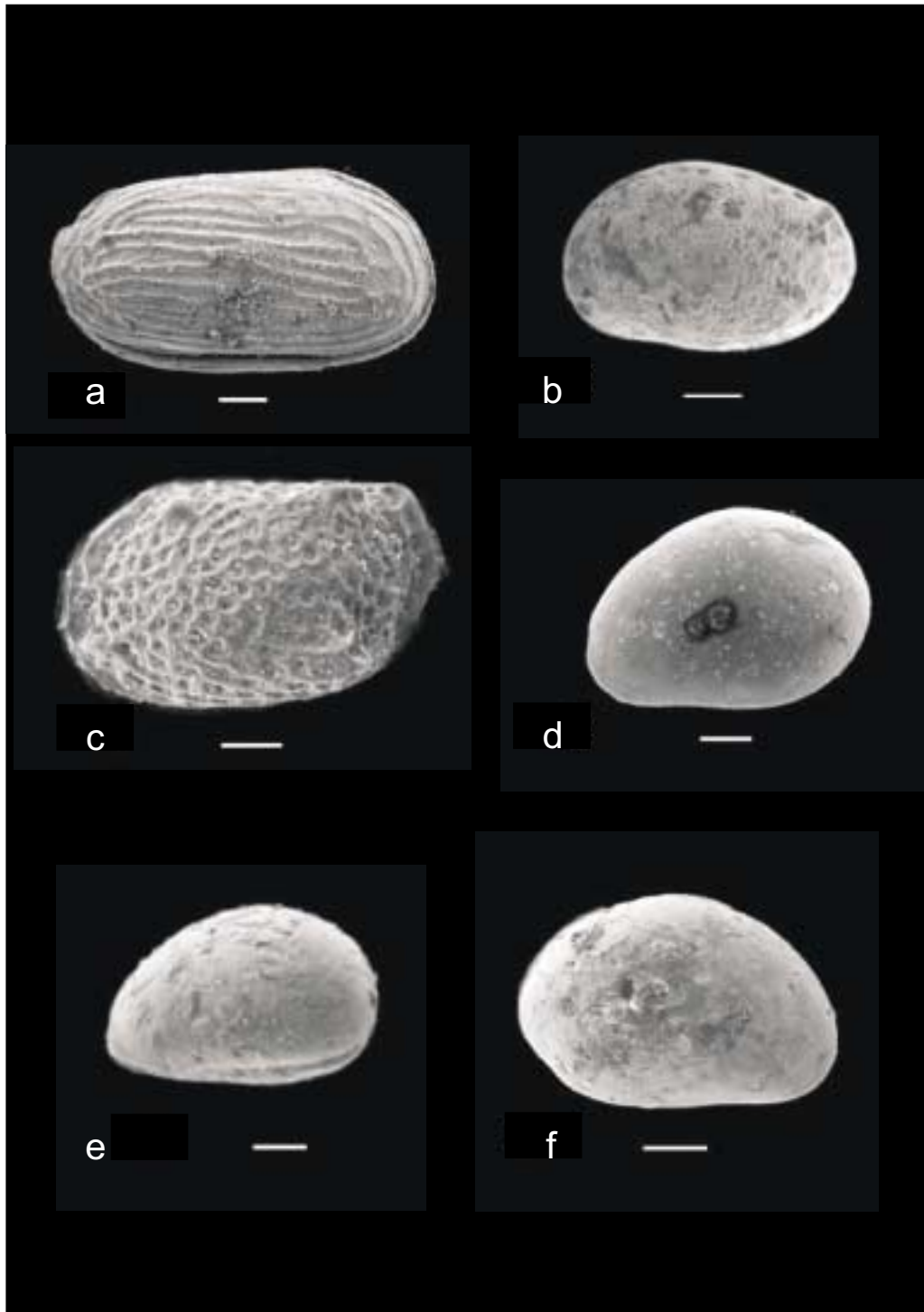


Figure 14. (a) *Cytheretta semiornata* (Egger), measured section at Sutaşı, Sample 1, carapace, right side view, scale bar 100 μm ; (b) *Hirshmannia viridis* (Müller), measured section at Sutaşı, Sample 8, carapace, left side view, scale bar 100 μm ; (c) *Loxoconcha alata* Brady, measured section Ortatepe, Sample 1, left valve, outside view, scale bar 100 μm ; (d) *Xestoleberis ventricosa* Müller, measured section Karalı, Sample 2, left valve, outside view, scale bar 100 μm ; (e) *Xestoleberis reymonti* Ruggieri, measured section at Sutaşı, Sample 2 carapace, left side view, scale bar 100 μm ; (f) *Xestoleberis communis* Müller, measured section at Sutaşı, Sample 8, right valve, outside view, scale bar 100 μm .

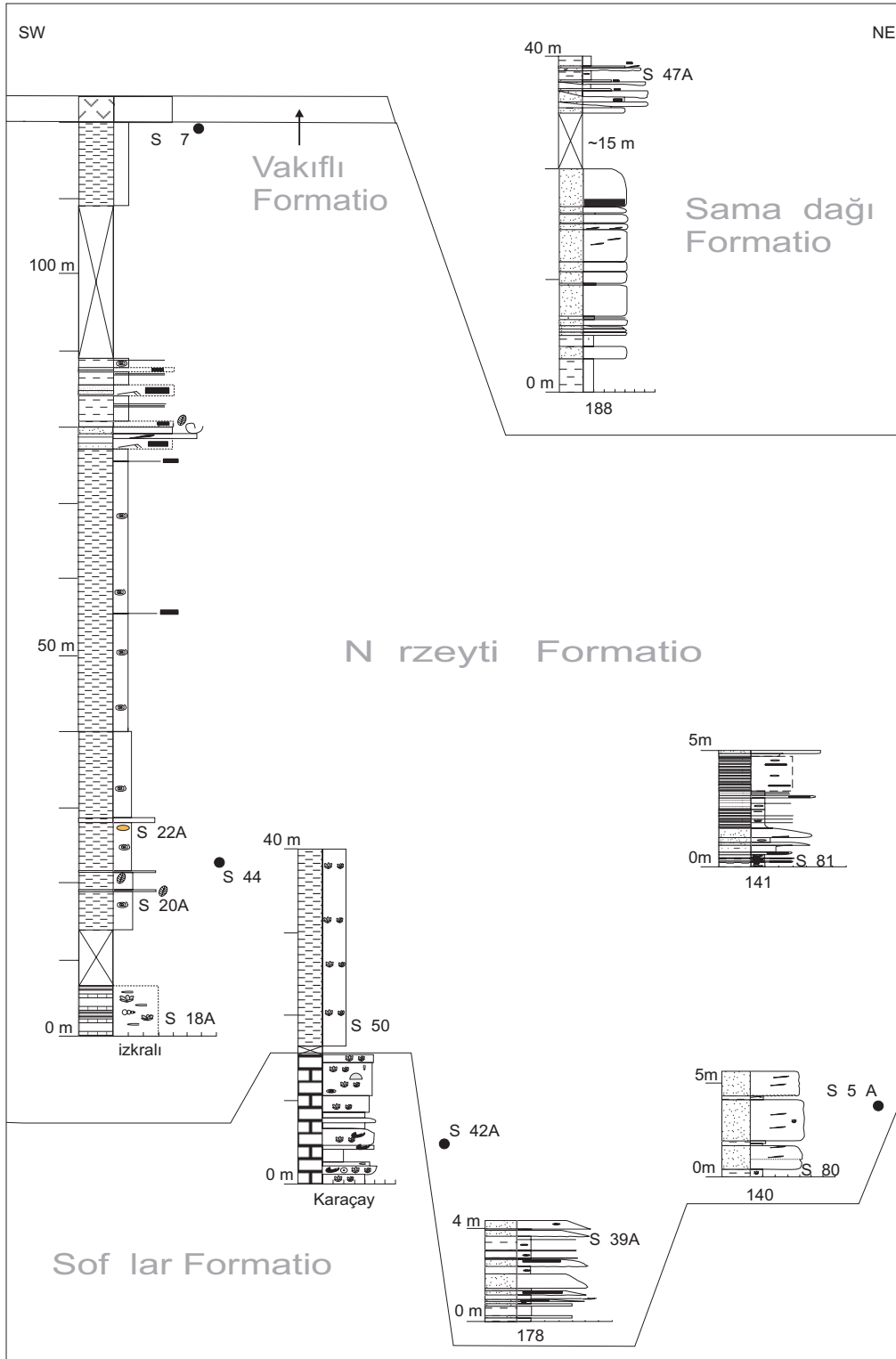


Figure 15. Figure showing stratigraphic columns for sections where samples for strontium analysis were collected; the location of the log is given at the base of each, either as a name or location number; see Figure 2 for their locations.

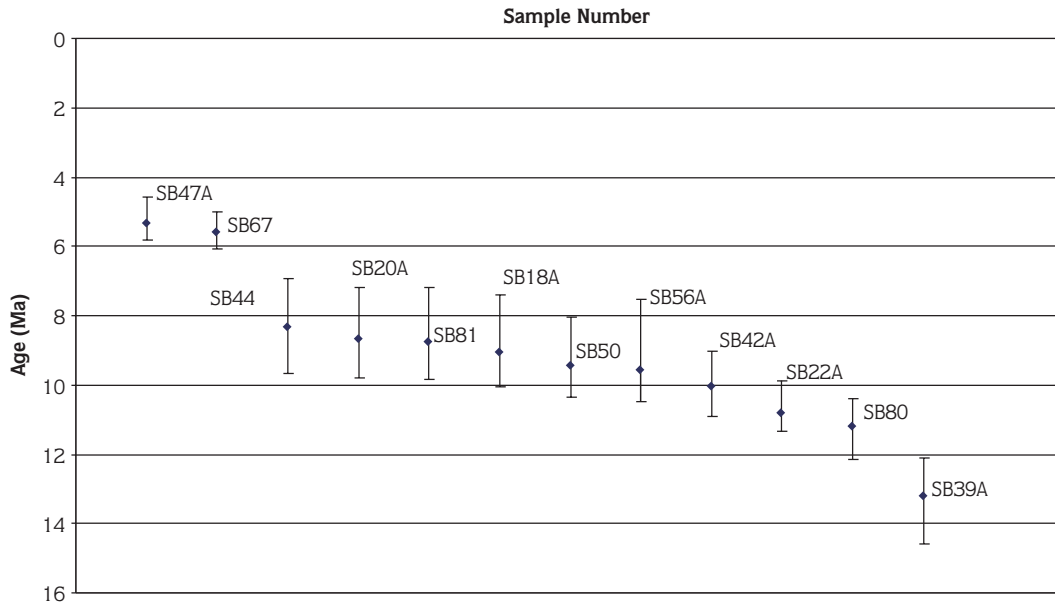


Figure 16. Graph showing the age ranges derived from strontium dating for each sample.

biomicrite-biosparite or wackestones, and fine-grained calcarenite. Beds are generally <50-cm thick with sharp bases and tops; ripples are developed on the surface of some beds. The limestones are rich in microfossils, especially large benthic foraminifera such as *Nummulites* sp. and orthophragmines together with macrofossils. However, much fossil material has been replaced by secondary calcite. Weathered surfaces of this unit are usually karstified. There is little variation within this formation, although Decrouez & Selçuk (1981) noted that the abundance of detrital material increases upwards and that it is also laterally variable.

Lower and Upper Boundaries (Figure 17): The base of the Okçular Formation can be observed to the east of Antakya (Figure 2). In some places the limestone directly overlies the Kızıldağ Ophiolite along an erosional surface; in other locations there is a complete sedimentary sequence and the base of the Okçular Formation is taken as the first limestone bed above a sequence of red and brown mudstones that forms the top of the underlying formation (Upper Cretaceous Kaleboğazı Formation). The contact between the Okçular and Kaleboğazı formations is conformable. The upper boundary of the Okçular Formation is unconformable with younger Neogene units.

Thickness and Regional Extent: The formation is regionally extensive, very similar to the Hacıdağı

Formation. The thickness of the unit has been estimated as 200–320 m (Selçuk 1981) but thicknesses of only 60–100 m were inferred during this study.

Previous Dating Evidence: The Okçular Formation corresponds to the lower part of the *Acarinina bulbrooki* (Bolli) biozone of Şafak (1993a), assigned to the Lutetian stage of the Eocene. The lower boundary is additionally defined by the first occurrence of *Turborotalia centralis* (Cushman and Bermudez) (Şafak 1993a). The ranges of *Morozovella aragonensis* and *Truncorotaloides topilensis* are entirely contained within the Okçular Formation (Şafak 1993a).

Kışlak Formation

Synonymy: This formation was defined by Atan (1969) and has been retained in the same sense by later workers.

Name and Type Location: The formation is named after the Kışlak village, 20 km south of Antakya. The type section is on the Antakya-Yayladağı road near the village.

Lithology: The lower part of the formation is composed of marls and marly limestones, whereas the upper part of the formation is made up of marls and calcarenites. The limestones are cream to white, fine- to

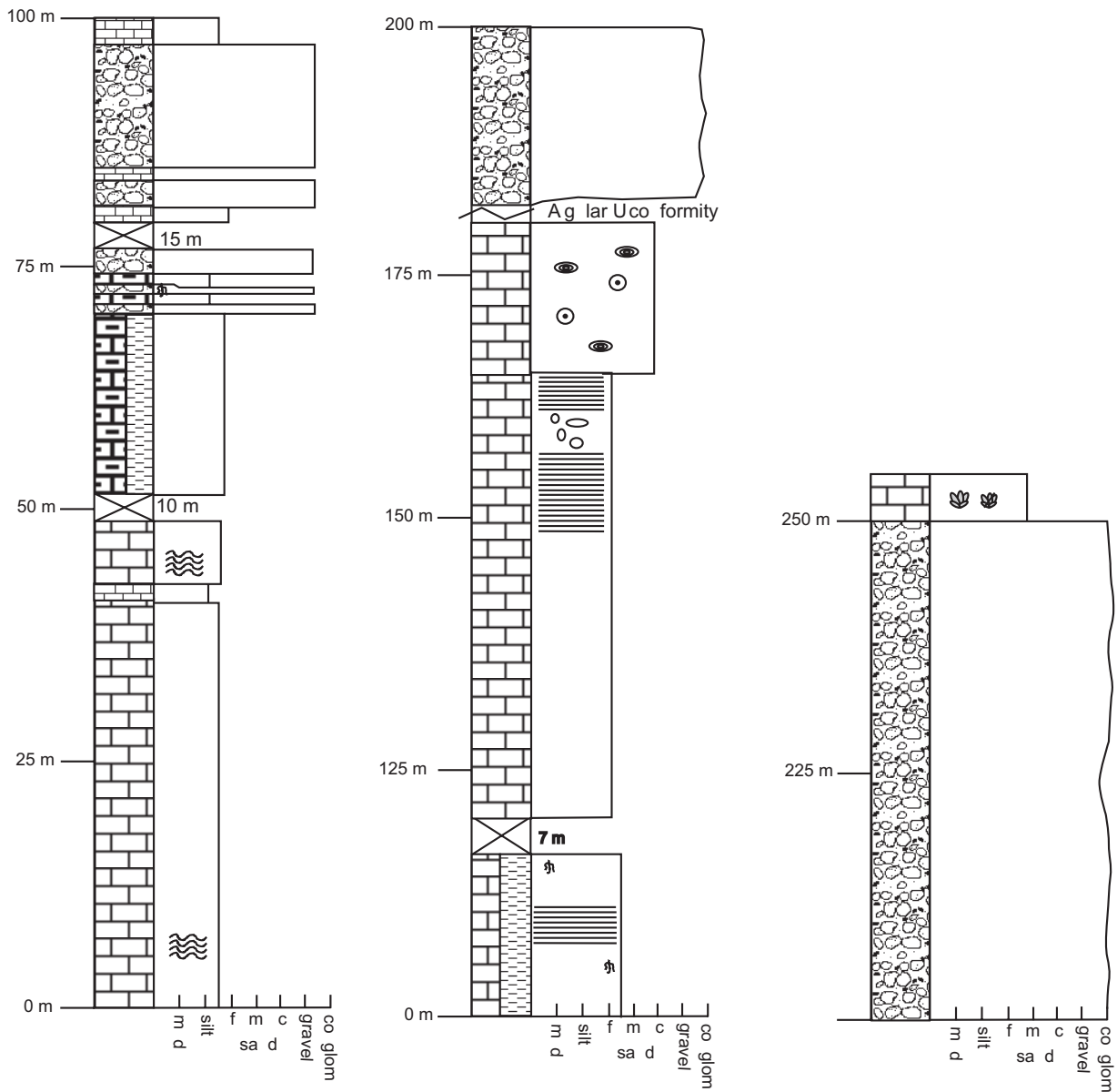


Figure 17. Sedimentary log of the Harbiye Gorge (Figure 2), showing the Kaleboğazı, Okçular, Balyatağı and Sofular formations and their mutual relationship.

medium-grained and fossiliferous, with both microfossils and macrofossils present.

Lower and Upper Boundaries: The lower boundary of the Kışlak Formation is transitional to the underlying Okçular Formation. The upper boundary is an unconformity with the Nurzeytin Formation.

Thickness and Regional Extent: The Kışlak Formation is only exposed in the south of the study area; further

north this formation is not present above the Okçular Formation and thus appears not to be laterally extensive. The thickness of the unit is 200–250 m (Selçuk 1981).

Previous Dating Evidence: The Kışlak Formation forms the upper part of the *Acarinina bullbrookii* biozone and contains *Morozovella spinulosa* and *Morozovella lehneri* (Şafak 1993a).

Table 8. Distribution of planktonic foraminifera and ostracods from the sections at Iskender Tepe (measured from 0232850/4005582, topological map Antakya P36-d1) and at Serinyol (measured from 0248123/4029755, topological map Antakya P36-a3).

Tertiary											SYSTEM	IS- ISKENDER TEPE	
Neogene													
Miocene					Late						SERIES		
Nurzeytin Formation											FORMATION		
1	2	3	4	5	6	7	8	9	10		SAMPLE NUMBER		
											OSTRACODA		
											Planktonic Foraminifers		
	+												<i>Globigerinoides trilobus</i> (Reuss)
							+	+	+	+			<i>Globigerinoides sacculifer</i> (Brady)
											O		<i>Globigerinoides bisphericus</i> Todd
	+		+		+								<i>Globigerinoides ruber</i> (d'Orbigny)
			+										<i>Globigerinoides obliquus</i> Bolli
			+										<i>Globigerinoides extremus</i> Bolli & Bermudez
							+	+	+	+			<i>Orbulina suturalis</i> Brönnimann
												+	<i>Globoquadrina dehiscens</i> (Chapman, Parr & Collins)
							+						<i>Globigerinella obesa</i> (Bolli)
Miocene					Middle						SR- Serinyol		
1	2	3	4	5	6	7	8	9	10	11			
						+			+				<i>Globigerinoides trilobus</i> (Reuss)
						+							<i>Orbulina suturalis</i>
						+							<i>Orbulina bilobata</i> (d'Orbigny)

O: reworked fossils

Balyatağı Formation

Synonymy: Enek Formation (in part), Pişkin *et al.* (1986), Selçuk (1981) and Atan (1969).

Name and Type Locality: The formation is named after Balyatağı Tepe, 1 km west of Enek village. The type section is exposed on the northwest side of the hill (Figure 2).

Lithology and Variation (Figure 18): The formation consists of interbedded lenticular matrix- and clast-supported conglomerates, coarse litharenites and mudstones of various colours i.e., cream, brown and red. The proportion of mudstone increases up-section and the clast size of the conglomerates generally decreases from a maximum size of >1 m near the base of the formation to a maximum size of <50 cm near the top. In the southeast the mudstones form a minor component of the

formation, only occurring as interbeds in the uppermost part of the succession. In the northwest, however, the upper part (~25 m) of the formation is composed entirely of mudstones.

Lower and Upper Boundaries: The base of the Balyatağı Formation varies from the north to the south. In the north, it overlies the Kızıldağ Ophiolite along an erosional surface. However, in the south the base of the formation is an angular unconformity with the Eocene Kışlak Formation. The upper boundary is a sharp contact between the Balyatağı Formation and the limestones of the Sofular Formation. This contact is locally variable and has been observed as being both conformable and with a slight angular unconformity.

Thickness and Regional Extent: The thickness of the formation is very variable; it is ~50-m thick in the type

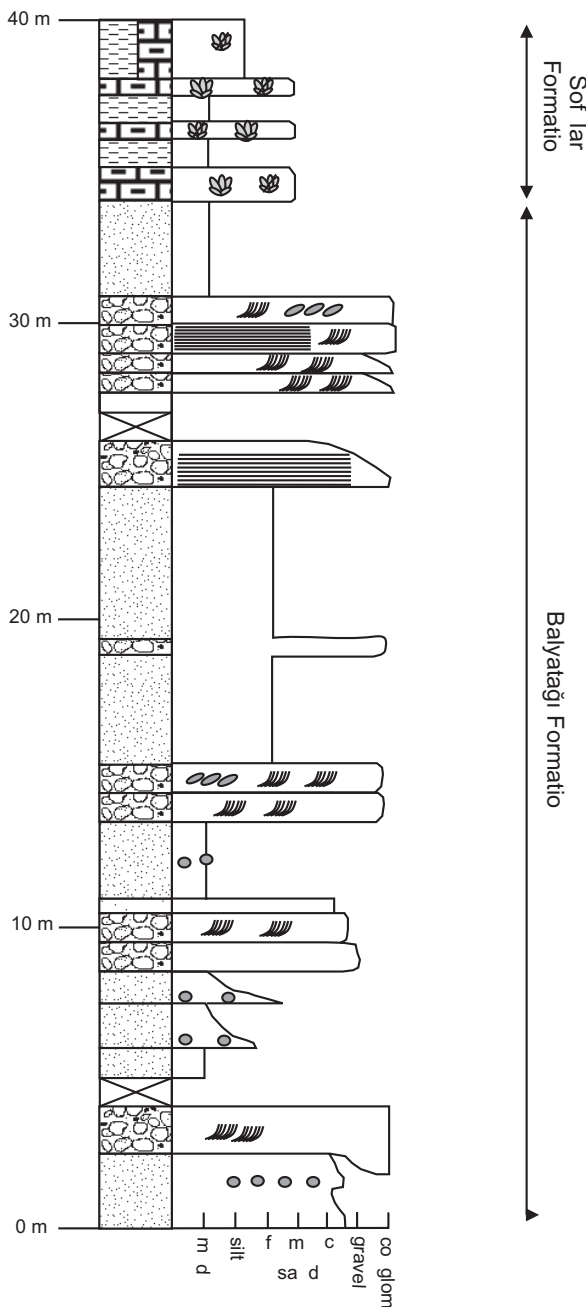


Figure 18. Sedimentary log of the Balyatağı Formation measured for the type location of Balyatağı Tepe, west of Enek (Figure 2).

section. To the northeast of the type locality the thickness increases to a maximum of ~175 m, whereas to the southeast the formation thickens to ~65 m, and then gradually disappears. In the northeast the formation thins to the south from >100 m to zero near the village of Ballıöz.

Previous Dating Evidence: The Balyatağı Formation is dated as Aquitanian to Burdigalian (Early Miocene) in age (Şafak 1993a). The base of the formation is marked by the first occurrence of *Globigerinoides trilobus*, which gives its name to the biozone. There is also the first occurrence of *Globigerinoides ruber* and *Globorotalia obesa*. Ostracods have been identified in the upper part of this formation, characterised by *Aurila soummamensis* (Şafak 1993b), also by the first occurrence of *Hemicyprideis helvetica* and *Falunia plicatula*. The appearance of *Cytherella vulgata* and *C. ramosa subalevis* indicate the position of the Aquitanian to Burdigalian boundary (Şafak 1993b). The top of the formation is marked by the last occurrence of *Cytheretta simplex* and *Cytheretta orthozensis* (Şafak 1993b).

Sofular Formation

Synonymy: Enek Formation (in part), Pişkin *et al.* (1986), Selçuk (1981) and Atan (1969). Sofular and Tepehan formations, Şafak (1993), Mistik (2002), Temizkan (2003).

Name and Type Locality: The formation is named after Sofular village, 10 km south of Antakya (Figure 2). The type location is exposed in a gorge system that runs WNW–ESE to the south of the village, as far as Kozkalesi village, 1.5 km away.

Lithology and Variation (Figure 19): In the type section the lower part of the formation comprises bioclastic calcirudites, mainly wackestones rich in shallow-marine fauna (i.e. bivalves, corals and echinoids). These limestones are massive-bedded and often muddy, with evidence of intense bioturbation. Cream-to-red mudstones are interbedded with the limestones; these beds have sharp bases, often capped by a thin conglomerate layer. Up-sequence, the mudstone beds disappear and the formation is composed entirely of bioclastic limestones. The formation shows little facies variation with most exposures consisting of calcirudites; however, in exposures along the River Asi, near Yeşilyazı village, the lower part of the succession consists of thin-bedded red and brown mudstones passing upwards into thin-bedded calcilutites. The upper part of the succession consists of bioclastic calcirudites and medium-grained calcarenites.

Lower and Upper Boundaries: The base of the formation is not exposed at the type section. In other areas the Sofular Formation was observed overlying the

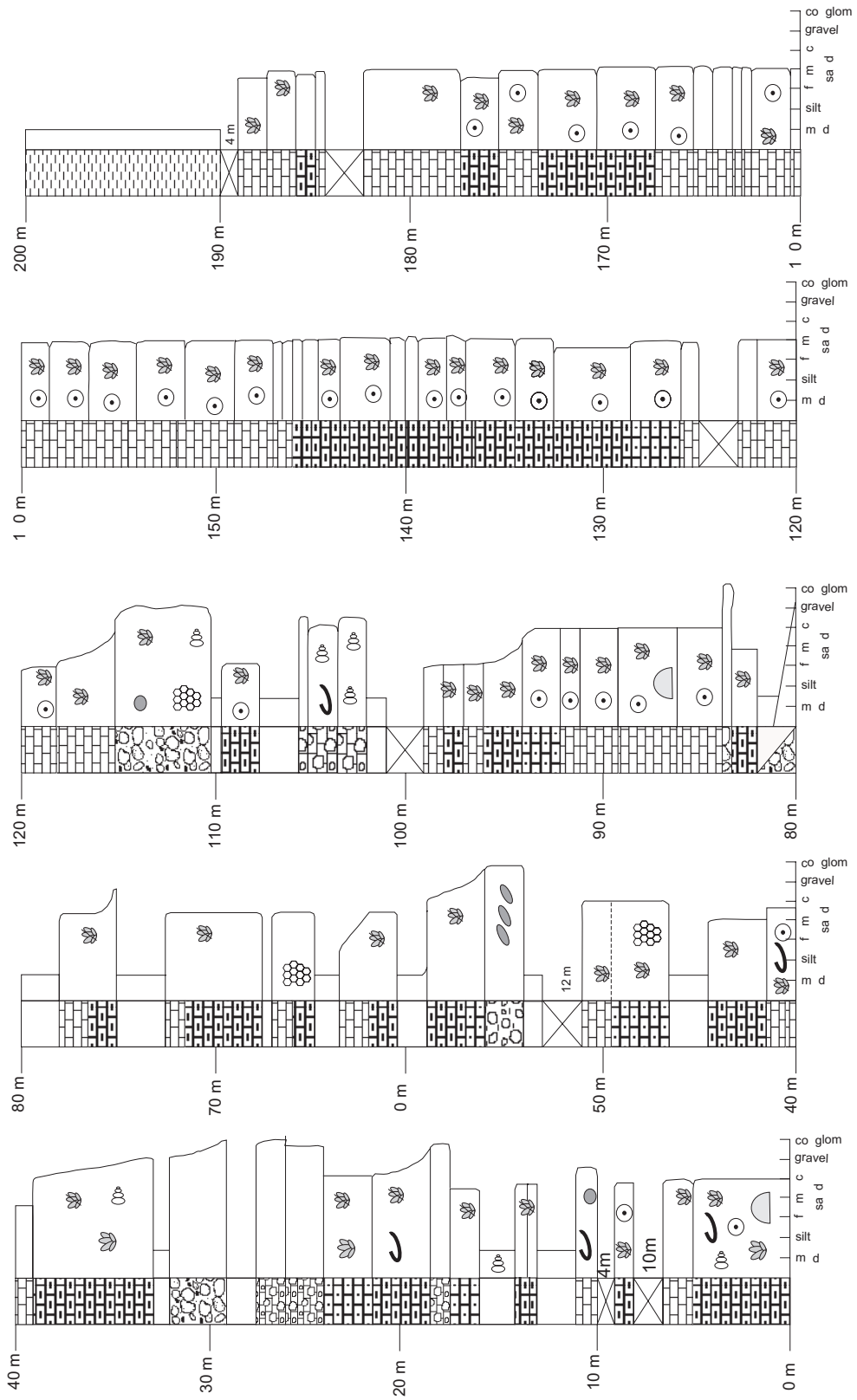


Figure 19. Sedimentary log of the Sofular Formation measured for the type location of this formation – Kozkalesi (Figure 2).

Kızıldağ Ophiolite, the Kışlak Formation or the Balyatağı Formation in different areas. The contact is sharp with an abrupt change in lithology from siliciclastic sediments to bioclastic limestones. The upper boundary is gradational, normally over several metres, and is defined as the level where marl of the Nurzeytin Formation dominates.

Thickness and Regional Extent: In the type area the Sofular Formation exceeds 200 m in thickness. Thick exposures of the formation crop out in coastal exposures and along the River Asi (Figure 2). The formation thins inland (to the northeast) on both margins of the basin until it eventually disappears.

Previous Dating Evidence: The Sofular Formation is dated as uppermost Burdigalian/base-Langhian to top-Langhian in age. It encompasses the whole of the planktonic foraminiferal biozones of *Praeorbulina glomerata* *curva* and *Orbulina suturalis* (Figure 8), which is equivalent to the whole of the ostracod biozone *Neomonoceratina helvetica* and the base of the *Carinocythereis* biozone (Şafak 1993a, b). The base is marked by the first occurrence of several ostracod species including *Cymocytheridea contracta* and *Cytherella petrosa*. The top of the formation is marked by the last occurrence of several ostracod species including *Cymocytheridea reversa* and *Falunia retiformis* and the planktonic foraminifer species *Globorotalia obesa* (Figure 10).

Nurzeytin Formation

Synonymy: Yazır Formation, Pişkin *et al.* (1986), Selçuk (1981) and Atan (1969).

Name and Type Locality: The formation is named after Nurzeytin village, 5 km north of Samandağı (Figure 2). The type section is located in the valley to the east of the village.

Lithology and Variation (Figure 20): The Nurzeytin Formation consists mainly of fossiliferous marls. Laterally discontinuous beds of sand, limestone and conglomerate are present within the marl sequence. Thick litharenite beds are more common in more northerly outcrops, often massive-bedded, although laminations and ripples are observed, together with thin chalk horizons and mud rip-up clasts. Thin sand horizons are found throughout the formation. Limestones are more common in the southerly outcrops, where flutes and grooves are observed on the base of beds. One metre-thick matrix-supported

conglomerate was observed, composed of marl clasts set in a marl matrix. The Vakıflı Member, composed of gypsum (selenitic and alabastrine gypsum), occasionally caps the top of this formation.

Lower and Upper Boundaries: The lower boundary is gradational with the underlying Sofular Formation and is diachronous based on the new strontium results. The upper boundary is poorly exposed but appears to be either conformable with the basal marl of the Samandağ Formation, or is marked by a gypsum horizon (Vakıflı Member).

Thickness and Regional Extent: The formation is laterally extensive, and is exposed both within and outside the present-day topographic basin. The maximum thickness is ~300 m; the upper gypsum horizon is exposed at five locations and varies in thickness from 5–25 m.

Previous Dating Evidence: The Nurzeytin Formation is dated as Serravallian to Tortonian, based on the recognition of the planktonic foraminiferal zone of *Orbulina universa* and the ostracod zones of *Carinocythereis* and *Cyprideis* (Şafak 1993a, b).

New Dating Evidence: The top of the formation can be recognised by the last appearance of the planktonic foraminifera *Orbulina bilobata* (*d'Orbigny*) (Figure 9), *Neogloboquadrina acostaensis* and *Globoquadrina venezuelana* and the last appearance of several ostracod species including *Aurila skalae*, *Aurila convexa* (Figure 12) and *Cyprideis anatolica*. Samples were taken for strontium dating from a number of intervals within the Nurzeytin Formation and these gave a range of ages from a maximum of 13.24 Ma to a minimum of 7.17 Ma, corresponding to Serravallian to Tortonian age.

Vakıflı Member

Synonymy: Vakıflı Formation, Şafak (1993a).

Name and Type Location: The Vakıflı Formation is named after the village of the same name to the north of Samandağı (Figure 2). The type section is ~ 1.5 km to the ENE.

Lithology and Variation: The type section is mainly composed of fine-grained alabastrine gypsum. This exposure includes large angular blocks (>2 m) of laminated alabastrine gypsum set in a gypsiferous marl matrix. In places, the alabastrine gypsum is seen to have

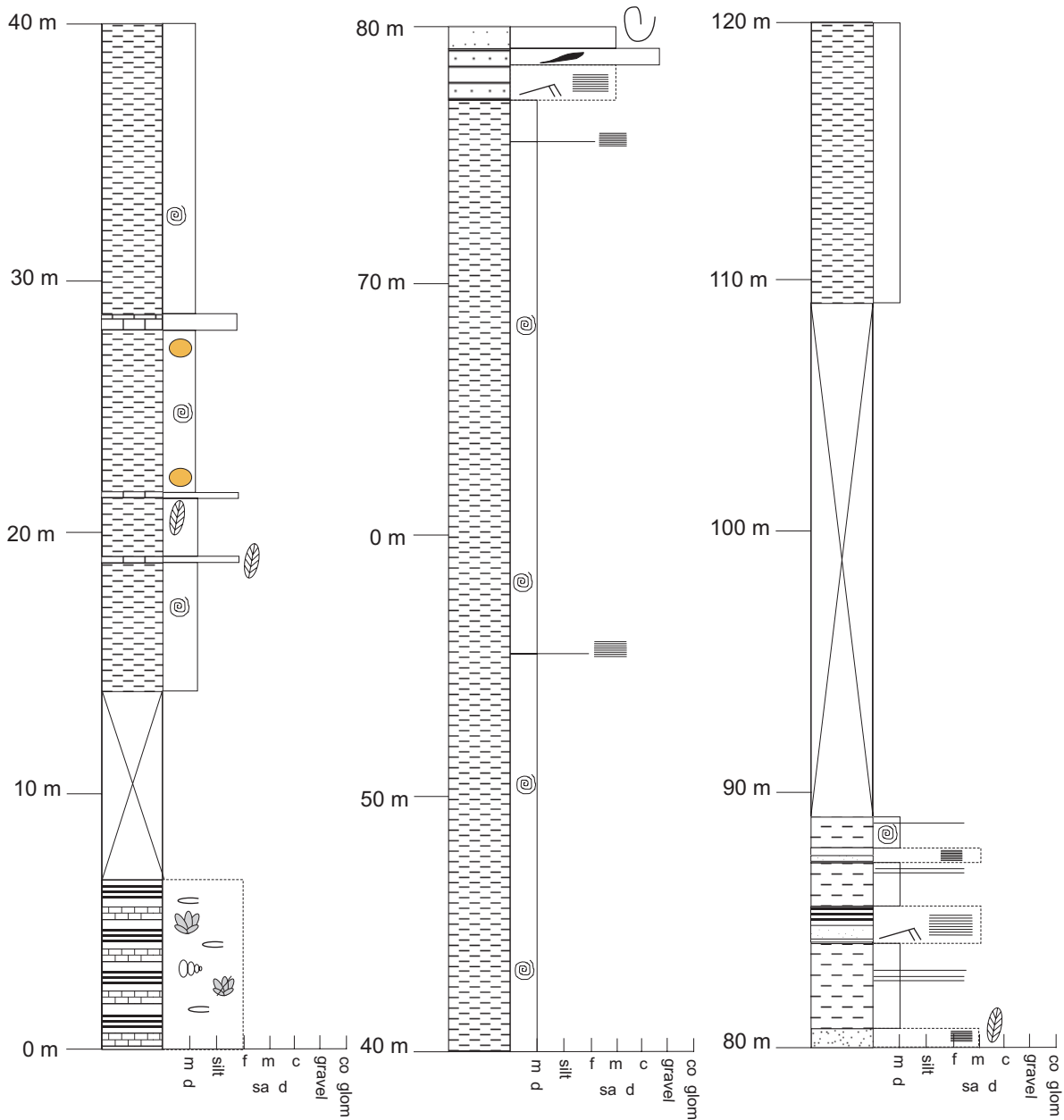


Figure 20. Sedimentary log of the Nurzeytin Formation (also shown in Figure 6), measured at its type location in Mizraklı valley, near the village of Nurzeytin (Figure 2).

undergone diagenetic alteration to coarse selenitic gypsum. Other exposures consist of coarse-grained selenitic gypsum, including one location where the basal gypsum is made up of banded selenite. This outcrop comprises repeated layers of selenite crystals, 1–5 cm in size. The overlying interval is composed of thick (>1 m), massive fragmented selenite crystals, 5 cm or more in

size. There are only isolated exposures of this member and both facies and microfossil evidence from this study indicates that in most cases there was no deposition during the Messinian.

Lower and Upper Boundaries: The lower boundary is conformable with the Nurzeytin Formation and the upper boundary is conformable with the Samandağ Formation.

Thickness and Regional Extent: The Vakıflı Formation has been identified in six locations in the field area; the thickest deposit (the type section) is 25 m thick with the other locations being in the order of 5–10 m thick.

Previous Dating Evidence: This formation is dated as Messinian in age based on the ostracod species, *Cyprideis ruggeri* and the presence of the planktonic foraminifer *Globoquadrina altispira altispira* at the very top of the formation (Şafak 1993a).

Samandağ Formation

Synonymy: Defined by Atan (1969); retained in the same sense by later workers.

Name and Type Locality: The Samandağ Formation is named after the Samandağ (mountain) and the adjacent town of the same name (Figure 2).

Lithology and Variation (Figure 6B): The lithology of lower part of the formation is dominated by fossiliferous marl, and is similar to the Nurzeytin Formation in field characteristics but the Samandağ Formation has a greater abundance of gastropods, is micaceous and contains more sand. Thin litharenite horizons are common; these are often laterally discontinuous, as are rare conglomerate horizons. Intraformational slumps and channel incisions are also observed. The upper part of the sequence is composed of fossiliferous and non-fossiliferous orange-weathering litharenites, which become generally coarser upwards. Locally, these sandstones contain stringers of shallow-marine fauna (mostly bivalves), cross-bedding and parallel laminations. Rare conglomerate lenses are present. The contact between the Lower and Upper Pliocene is transitional.

Lower and Upper Boundaries: The lower boundary is rarely exposed, but it was observed conformably overlying the Nurzeytin Formation. At one location the Samandağ Formation overlies an erosion surface cut into the Sofular Formation.

Thickness and Regional Extent: No complete section is exposed and regional faulting affects the formation. The estimated thickness of the Samandağ Formation is 100–400 m. The formation is only exposed within the present topographic basin, towards the coast.

New Dating Evidence: The base of the Pliocene is characterised by the first appearance of the planktonic foraminifera *Globigerinoides trilobus sacculifer*,

Globigerinoides obliquus obliquus and *Globorotalia scitula*. One sample provided a Pliocene date using strontium analysis, giving a date of 5.35 Ma.

Lithostratigraphic Units of the Kırıkhan Area

Hacıdağı Formation

Synonymy: Kocagedik Formation, Yılmaz (1982); Cona Formation (in part), Kozlu (1982). Amalgamated into the Cona Formation in the Osmaniye area by Yılmaz *et al.* (1984).

Name and Type Location: The type location of the Hacıdağı Formation is to the northwest of Kaypak (Serdar) town near the city of Osmaniye (Günay 1984).

Lithology and Variation: The Hacıdağı Formation is composed of white calcarenites and limestone. Beds are generally <50-cm thick and contain foraminiferal lags, bioturbation and fine laminations. Many beds also exhibit normal grading and chert nodules, mostly within the upper parts of beds. Intraformational slumps have been recognised, but overall there is very little variation in lithology.

Lower and Upper Boundaries: The lower boundary is transitional to the underlying Cona Formation. The upper boundary is marked by an angular unconformity with the Kıcı Formation.

Thickness and Lateral Extent: The formation is laterally extensive and >400-m thick. The thickness is difficult to estimate as the formation has been extensively folded.

Previous Dating Evidence: The Hacıdağı Formation is rich in microfossils, which date the formation as Palaeocene to Eocene in age. Benthic foraminifera include *Discocyclus archiaci*, *Alveolina rutimeeri*, *Assilina cf. laminose* (Gill) and Planktic foraminifera *Globorotalia velascoensis* (Atan 1969).

Kıcı Formation

Synonymy: Gildirli Formation, Derman (1979); Enek Formation (Sofular Member), Selçuk (1981); Kalecik Formation (Horu limestone Member), Kozlu (1982).

Name and Type Location: The Kıcı Formation is named after Kıcı village on the Antakya-Belen road (Figure 4). The Kurthisoğuksu section is here recognised as the new type location.

Lithology and Variation (Figure 21): The lower part of the formation is composed of thick matrix-supported conglomerates composed of large angular, to sub-rounded clasts of limestone, basalt and sandstone. The upper part of the sequence is composed of red-purple conglomerates and coarse litharenites, with occasional dark grey and black mud horizons. The sandstones are cross-bedded and parallel laminated; bioturbation is common. There is some facies variation as the basal conglomerates are only locally developed.

Lower and Upper Boundaries: The lower boundary of the Kıcı Formation is a sharp angular unconformity with

the underlying Hacıdağı Formation. The upper boundary is also a sharp unconformity with the Kepez Formation, or the Gökdere Formation.

Thickness and Lateral Extent: The Kıcı Formation is only observed around the Kırıkhan area and is ~100–150- m thick.

Dating Evidence: No published evidence. Based on similarities with the Hatay Graben the Kıcı Formation is correlated with the Balyatağı Formation and thus has an Aquitanian to Burdigalian age (Şafak 1993a).

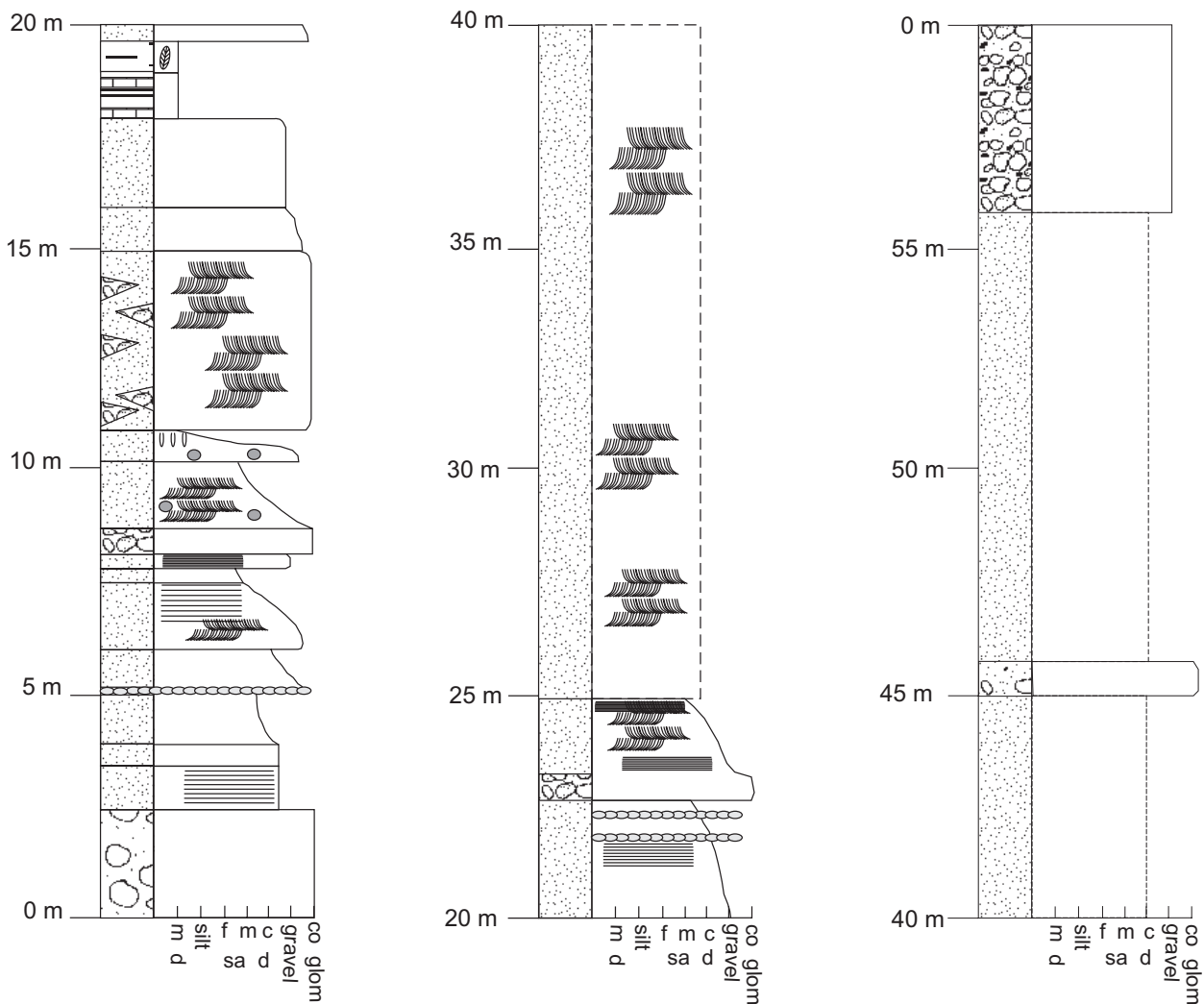


Figure 21. Sedimentary log of the Kıcı Formation measured at the type location of this formation – Kurthisoğuksu, 2 km east of Kıcı (Figure 11).

Kepez Formation

Synonymy: Karaisalı Limestone, Derman (1979); Enek Formation, Selçuk (1981); Kalecik Formation, Kozlu (1982), Teknepınar Formation, Günay (1984).

Name and Type Locality: This formation is named after Kepez Tepe (also the type locality), 6 km west of Kırıkhan.

Lithology and Variation: The Kepez Formation is composed of white biosparite and bimicrite. The bioclastic material is completely fragmented, but coral, bivalves and echinoids have been recognised. The formation is poorly exposed and is usually karstified. There is little lithological variation in the observed outcrops.

Lower and Upper Boundaries: The lower boundary is a sharp unconformity with the Kıcı Formation. The upper boundary is a lateral and vertical transition with the Gökdere Formation.

Thickness and Lateral Extent: The formation is restricted in extent, as it is only exposed on a two hill-tops near Gökdere village and just to the southwest of Kırıkhan (Figure 4), where it is exposed probably due to faulting. The maximum thickness is estimated as ~345 m (Derman 1979) but in the field the maximum observed thickness is ~15 m.

Dating Evidence. No published evidence. Based on similarities with the Hatay Graben the Kepez Formation can be correlated with the Sofular Formation, suggesting a Langhian (Middle Miocene) age.

Gökdere Formation

Synonymy: Arbo Formation, Bryant (1960); Seyhan Formation, Derman (1979); Enek and Yazır Formation, Kozlu (1982); Altınözü Formation, Günay (1984).

Name and Type Location: The Gökdere Formation is named after Gökdere village, 5 km west of Kırıkhan (Figure 4). The type section is exposed along the Gökdere-Kırıkhan road to the SE of the village.

Lithology and Variation (Figure 22): The Gökdere Formation is dominated by marl, although there is a significant amount of litharenite. The sandstones typically form several metre-thick units. Two main types of sand body were observed: (i) thin sandstone beds, interbedded with marl, containing plant material and abundant *Ostrea*,

also ripples and flutes, and (ii) thicker sandstone beds without marl interbeds, although ripples and load-casts are present. Although the marl is laterally continuous the sandstones tend not to be. Sandstone predominates near the top of the formation.

Lower and Upper Boundaries: The lower boundary is unconformable on the Kıcı Formation, or conformable on the Kepez Formation. The top of the formation is usually marked by an erosional surface with Quaternary alluvium above.

Thickness and Lateral Extent: The formation is laterally extensive and very thick (up to 700 m); at the type location it is ~ 430 m thick.

Previous Dating Evidence: The presence of the ostracods *Cyprideis seminulum* and *C. antolica* indicate that this formation is Tortonian to Messinian in age (Kozlu 1982). Samples were collected for micropalaeontological analysis from the type section during this study, but age-diagnostic taxa were not found.

Interpretation of Stratigraphical Relations

The sedimentary rocks of the Hatay Graben and the Karasu Rift, in the area around Belen and Kırıkhan, record a change from regional shelf deposition on the periphery of a foreland basin related to the Tauride (Misis-Andırın) Suture Zone in the north, to a more active tectonic regime influence by the “tectonic escape” of Anatolia (Boulton *et al.* 2006). A great variety of sub-environments developed during the Pliocene and Pleistocene (Boulton 2006).

The Okçular, Kışlak, Cona and Hacıdağı formations record carbonate deposition on a shallow-marine shelf that covered the whole area during latest Cretaceous to Eocene times (Figure 23). This period of deposition was followed, in the Oligocene, by a widespread hiatus linked to relative sea-level fall, probably as a result of regional continental collision to the north along the Misis-Andırın Suture Zone, and its eastward extension as the Bitlis Suture Zone (Robertson *et al.* 2004). This regional collision caused flexural uplift to the south and folding of the Eocene and older sediments; after this hiatus, the sedimentary record resumed in the Burdigalian.

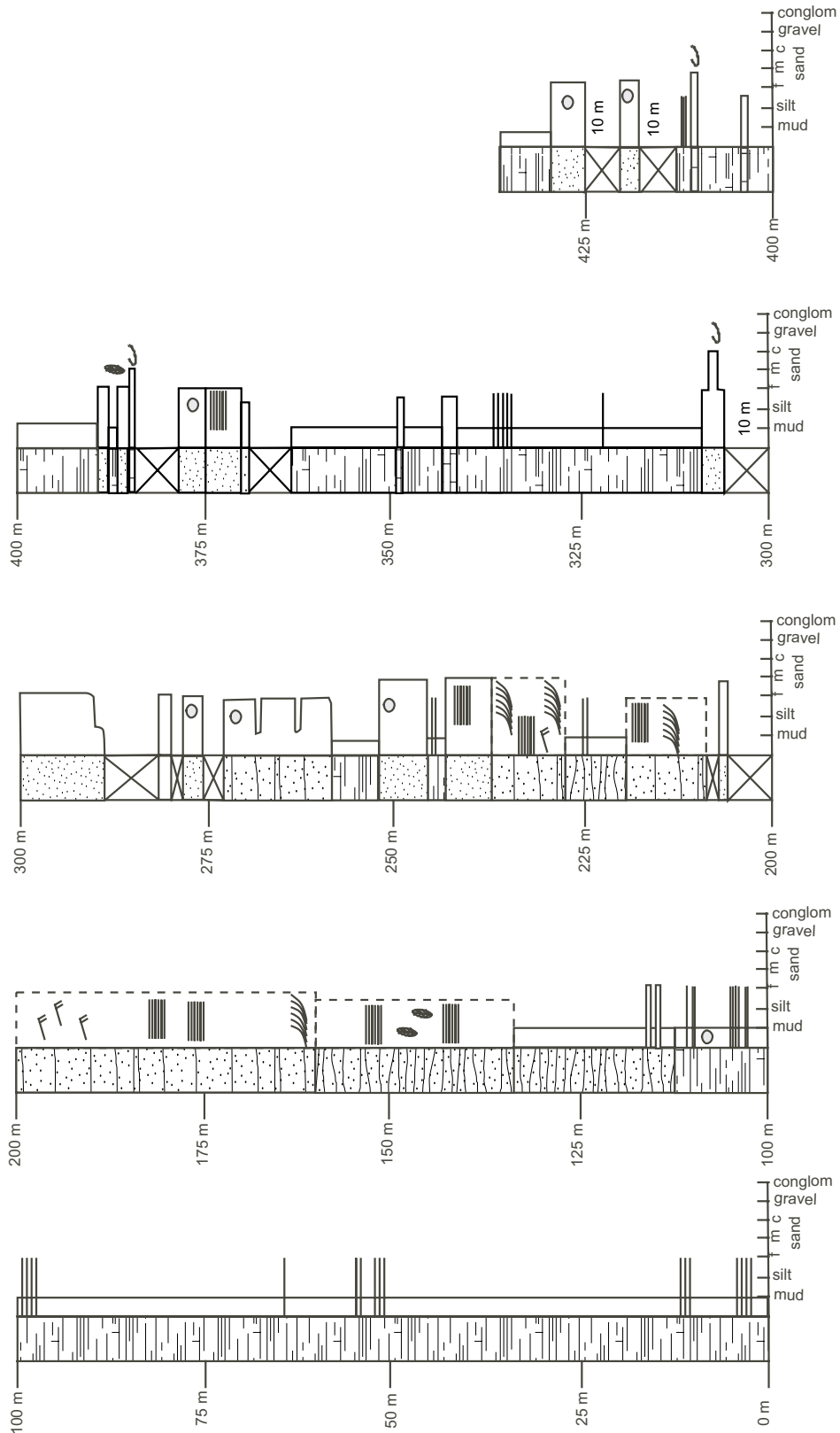


Figure 22. Sedimentary log of the Gökdere Formation measured at the type location for this formation – Gökdere (Figure 4).

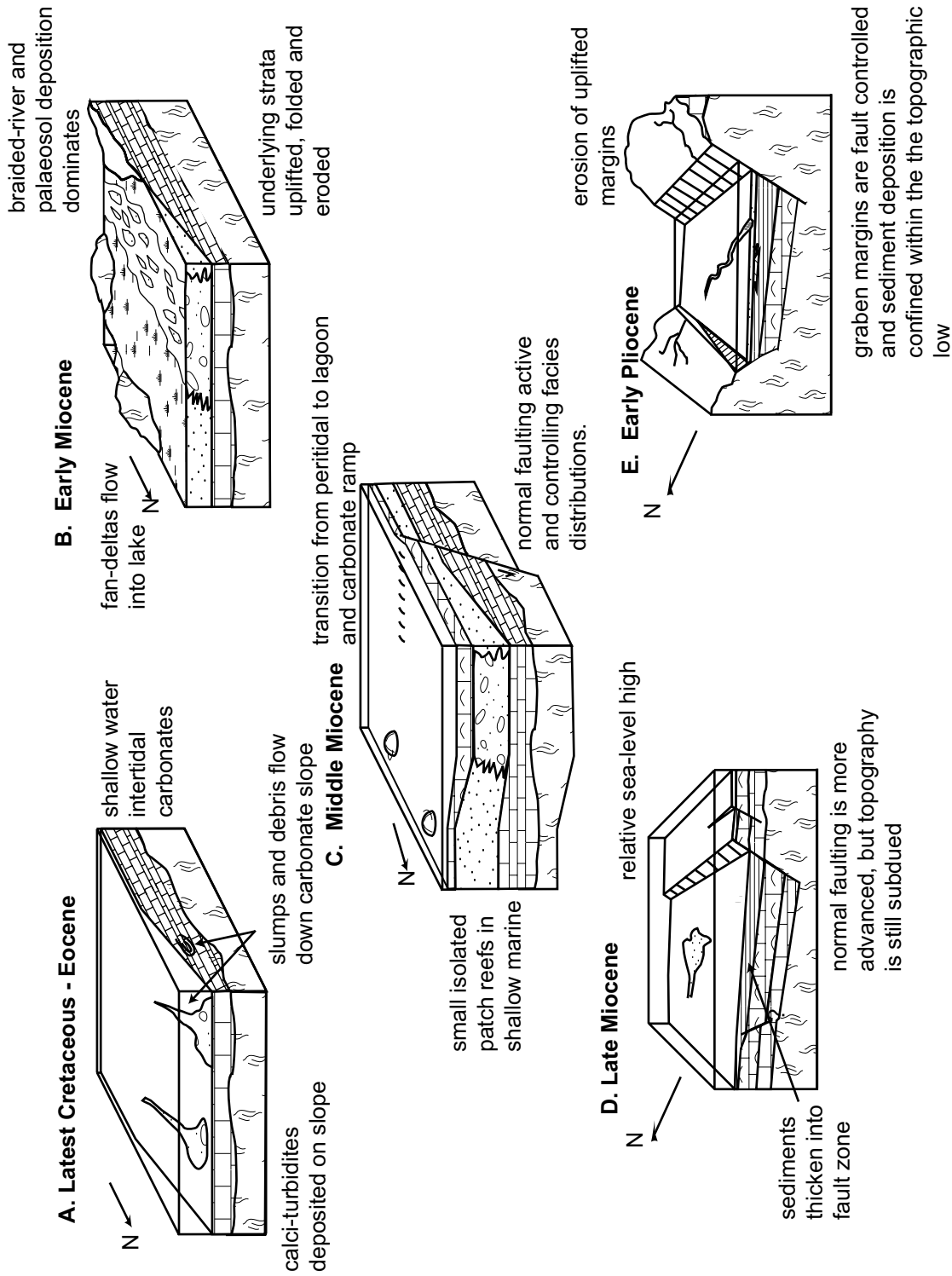


Figure 23. Simplified block diagrams illustrating the local geological evolution of the Hatay Graben from the Latest Cretaceous/Eocene to the Early Pliocene.

The Balyatağı Formation of the Hatay Graben is generally a fining-upward sequence of polymict conglomerates and sandstones that pass upwards into sandstones and mudstones (Boulton & Robertson 2007). These sediments are interpreted to represent gravel-rich braided river deposits that became more channelised over time, perhaps reflecting a reduction in relief in the source area that is inferred to have lain to the south (Boulton 2006; Figure 23). The Kıcı Formation is also continentally derived; however, the coarse lower conglomerates are likely to represent alluvial fan debris that fine up into delta plain and distributary mouth-bar sediments (Boulton 2006).

The Sofular and Kepez formations represent a return to shallow-marine carbonate deposition during the Langhian (Figure 23). The greater thickness of the Sofular Formation in the Hatay Graben area, suggests that greater accommodation space was available there at this time compared to areas to the northeast, or that the Kepez Formation has subsequently undergone significant erosion (Boulton 2006).

Subsequently, the Nurzeytin and Gökdere formations record progressive deepening of the area during the Serravallian to Tortonian (Figure 23). This reflects a continuing relative sea-level, rise probably related to loading of the continental lithosphere to the north as continental collision intensified (Boulton 2006; Boulton & Robertson 2007). Sandstone beds in the upper part of the Gökdere Formation are possibly representative of pro-delta deposits, suggesting that the area around Kırıkhan was shallower than the Hatay Graben during this time. Messinian evaporites and Pliocene sediments occur only within the elongate Hatay Graben. This is probably because the Karasu Rift further north had become fully continental before this time and thus did not undergo evaporite deposition during the Messinian salinity crisis. By the Messinian the tectonic regime in the area was changing from one of continental collision to one of 'tectonic escape', with the related formation of large strike-slip faults and an accentuated topographic relief (Boulton *et al.* 2006). During the Pliocene the Hatay Graben was characterised by shallow-marine environments (Figure 23) until the Late Pliocene to Quaternary when the area finally became non-marine in response to relative sea-level fall (Boulton 2006).

Conclusions

The stratigraphic nomenclature of the Hatay Graben and Karasu Rift is here redefined and simplified in order to aid correlation in a regional context. This has been achieved by using a combination of new strontium dating, micropalaeontology and field observations. The lithostratigraphy can be summarised as follows:

- Palaeogene units: the Cona Formation and the Hacıdağ Formation of the Karasu Rift in the north correlate with the Okçular Formation and the Kışlak Formation of the Hatay Graben in the south.
- Neogene units: The Lower Miocene Balyatağı Formation of the Hatay Graben is equivalent to the Kıcı Formation of the Karasu Rift. The Sofular Formation in the south is equivalent to the Kepez Formation in the north. Also, the Nurzeytin Formation in the Karasu Rift is equivalent to the Gökdere Formation in the Hatay Graben.
- The Tepehan Formation (Şafak 1993a) is now redundant in view of its lithological similarity with the Nurzeytin Formation.
- The Vakıflı Formation of Şafak (1993a) is downgraded to member status owing to its limited extent and small thickness. This member is present only in the Hatay Graben.

Finally, the new stratigraphy is intended to provide a rigorous framework for future work in this important region.

Acknowledgments

SJB acknowledges receipt of a NERC PhD Studentship (NER/S/A/2002/10361) and additional funding by the American Association of Petroleum Geologists for financial support. AHFR thanks the Carnegie Trust for the Scottish Universities for financial assistance with fieldwork. We also thank two anonymous reviewers for their comments, which enhanced this paper. We thank Jodie Fisher for help using the SEM.

References

- ATAN, O.R. 1969. *Eğribucak-Kırıkhan Bölgesindeki Ofiyolitlerin Jeolojisi ve Petrografisi [Geology and Petrography of the Eğribucak-Kırıkhan District Ophiolite]*. Mineral Research and Exploration Institute (MTA) of Turkey Publication no. 150 [in Turkish, unpublished].
- AVŞAR, N. 1991. *Osmaniye (Adana) Yöresi Üst Kretase Mestrihtiyen Bentik Foraminifer Faunası [Upper Cretaceous Maastrichtian Benthic Foraminifera Fauna of the Osmaniye (Adana) Area]*. Mineral Research and Exploration Institute (MTA) of Turkey Report no. 113 [in Turkish, unpublished].
- BOULTON, S.J. 2006. *Tectonic-sedimentary Evolution of the Cenozoic Hatay Graben, South Central Turkey*. Ph.D Thesis, University of Edinburgh, U.K. [unpublished].
- BOULTON, S.J. & ROBERTSON, A.H.F. 2007. The Miocene of the Hatay area, S Turkey: transition from the Arabian passive margin to an underfilled foreland basin related to closure of the Tethys Ocean. *Sedimentary Geology*. Doi:10.1016/j.sedgeo.2006.12.001
- BOULTON, S.J., ROBERTSON, A.H.F. & ÜNLÜGENÇ, U. 2006. Tectonic and sedimentary evolution of the Cenozoic Hatay Graben, Southern Turkey: A two-phase, foreland basin then transtensional basin model. In: ROBERTSON, A. H.F. & MOUNTRAKIS, D. (eds), *Tectonic Development of the Eastern Mediterranean*. Geological Society, London, Special Publications 260, 613–634.
- BRASS, G.W. 1976. The variation of marine $^{87}\text{Sr}/^{86}\text{Sr}$ ration during Phanerozoic time: Interpretation using a flux model. *Geochemical Cosmochemical Acta* 40, 721–730.
- BROEKER, W.S. & PENG, T.H. 1982. *Tracers in the Sea*. Eldigio, Pallisades, NewYork.
- BRYANT, G. 1960. *Stratigraphic Report on the Hassa Area, Petroleum District VII, Southeast Turkey*. American Overseas Petroleum Ltd, Report number 506.
- DECROUZE, D. & SELÇUK, H. 1981. Les Nummulites de la craie de la Formation d'Okçular (Hatay, unité tectonique des plis bordiers, sud de la Turquie). *Notes du Laboratoire de Palaeontologie de l'Université de Genève* 8, 7–18.
- DERMAN, A.S. 1979. *Antakya (Hatay) Civarı Stratigrafi ve Jeolojisi [Stratigraphy and Geology of the Hatay Region]*. TPAO (Turkish Petroleum Corporation) Report no. 1513 [in Turkish, unpublished].
- DUBERTRET, L. 1939. Sur la genèse et l'âges des roches vertes syreennes. *Comptes Rendus de l'Academie des Sciences, Paris* 209, p. 763.
- DUBERTRET, L. 1953. Géologie des roches vertes du nord-ouest de la Syrie et du Hatay (Turquie). *Notes et Mémoires sur le Moyen-Orient, Museum Nationale d'histoire naturelle* 5, 5–179, Paris.
- ELDERFIELD, H. 1986. Strontium isotope stratigraphy. *Palaeogeography Palaeoclimatology Palaeoecology* 57, 71-90.
- FLECKER, R. 1995. *Miocene Basin evolution of the Isparta Angle, Southern Turkey*. PhD Thesis, University of Edinburgh, U.K. [unpublished].
- FLECKER, R. & ELLAM, R.M. 2006. Identifying Late Miocene episodes of connection and isolation in the Mediterranean-Paratethyan realm using Sr isotopes. *Sedimentary Geology* 188, 189–203.
- FLECKER, R., DE VILLIERS, S. & ELLAM, R.M. 2002 Modelling the effect of evaporation on the salinity-Sr-87/Sr-86 relationship in modern and ancient marginal-marine systems: the Mediterranean Messinian Salinity Crisis. *Earth and Planetary Science Letters* 203, 221–233.
- FREUND, R., ZAK, I. & GARFUNKEL, Z. 1968. On the age and rate of sinistral movement along the Dead Sea rift. *Nature* 220, 253–255.
- GLEASON, J.D., MOORE, T.C., REA, D.K., JOHNSON, T.M., OWEN, R.M., BLUM, J.D., HOVAN, S.A. & JONES, C.E. 2002. Ichthyolith strontium isotope stratigraphy of a Neogene red clay sequence: calibrating aeolian dust accumulation rates in the central North Pacific. *Earth and Planetary Letters* 202, 625–636.
- GÜNAY, Y. 1984. *Amanos Dağlarının Jeolojisi ve Karasu-Hatay Grabeninin Petrol Olanakları [Geology of the Amanos Mountains and Petroleum Potential of the Karasu-Hatay Graben]*. TPAO (Turkish Petroleum Corporation) report on Hakkari-Şaryaj Project [in Turkish, unpublished].
- HEDBERG, H.D. (ed) 1976. *International Stratigraphic Guide*. Wiley, New York.
- HODELL, D.A. 1994. Progress and paradox in strontium isotope stratigraphy. *Palaeoceanography* 9, 395–398.
- HODELL, D.A. & WOODRUFF, F. 1994. Variations in the strontium isotopic ration of seawater during the Miocene: stratigraphic and geochemical implications. *Palaeoceanography* 9, 405–426.
- HOWARTH R.J. & McARTHUR, J.M. 1997 Statistics for strontium isotope stratigraphy: a robust LOWESS fit to the marine Sr-isotope curve for 0-206 Ma, with look-up table for derivation of numeric age. *Journal of Geology* 105, 441–456.
- KOP, A. 1996. *Kırıkhan ve Kuzeyinin Tektono-stratigrafik İncelemesi [Tectono-stratigraphic Investigations of Kırıkhan and its Northern Area]*. MSc Thesis, University of Çukurova [in Turkish with English abstract, unpublished].
- KOZLU, H. 1982. *İskenderun Baseni Jeolojisi ve Petrol Olanakları [Geology and Petroleum Potential of the Iskenderun Basin]*. TPAO (Turkish Petroleum Corporation) Report no. 1921 [in Turkish, unpublished].
- McARTHUR, J.M. 1994. Recent trends in strontium isotope stratigraphy. *Terra Nova* 6, 331–358.
- McARTHUR, J.M., HOWARTH, R. A.J. & BAILEY, T.R. 2001. Strontium Isotope Stratigraphy: LOWESS Version 3: Best Fit to the Marine Sr-Isotope Curve for 0–509 Ma and Accompanying Look-up Table for Deriving Numerical Age. *Journal of Geology* 109, 155–169.
- MILLER, K.G., FEIGENSON, M.D., WRIGHT, J.D. & CLEMENT, B.M. 1991. Miocene isotope reference section, Deep Sea Drilling Project Site 608: An evaluation of isotope and biostratigraphic resolution. *Palaeoceanography* 6, 33–52.

- MISTIK, T. 2002. *Samandağ (Antakya) Civarının Jeolojik İncelemesi [Geological Investigation of the Samandağ Area]*. MSc Thesis, Çukurova University [in Turkish with English abstract, unpublished].
- MURPHY, M.A. & SALVADOR, A. (eds) 1999. International Stratigraphic Guide – An Abridged Version. *Episodes* **22**, 255–271.
- OSLICK, J.S., MILLER, K.G., FEIGENSON M.D. & WRIGHT, J.D. 1994. Oligocene – Miocene strontium isotopes: stratigraphic revisions and correlations to an inferred glacioeustatic record. *Palaeoceanography* **9**, 427–443.
- PIŞKIN, O., DELALOYE, M., SELÇUK, H. & WAGNER, J. 1986. Guide to Hatay Geology (SE Turkey). *Ofioliti* **11**, 87–104.
- RICHTER, F.M. & DEPAULO, D.J. 1988. Diagenesis and strontium isotope evolution of sea-level using data from DSDP 590B and 575. *Earth and Planetary Science Letters* **90**, 382–394.
- ROBERTSON, A.H.F., ÜNLÜGENÇ, U.C., İNAN, N. & TASLI, K. 2004. The Misis-Andırın Complex: a Mid-Cenozoic melange related to late-stage subduction of the Southern Neotethys in S Turkey. *Journal of Asian Earth Sciences* **22**, 413–453.
- ROJAY, B., HEIMANN, A. & TOPRAK, V. 2001. Neotectonic and volcanic characteristics of the Karasu fault zone (Anatolia, Turkey): the transition zone between the Dead Sea transform and the East Anatolian fault zone. *Geodinamica Acta* **14**, 197–212.
- ŞAFAK, Ü. 1993a. Antakya Havzası planktonic foraminifer biyostratigrafisi [Planktonic foraminifera biostratigraphy of Antakya Basin]. *Proceedings of A. Suat Erk Geology Symposium*, 143–156 [in Turkish with English abstract, unpublished].
- ŞAFAK, Ü. 1993b. Antakya Havzası ostrakod foraminifer biyostratigrafisi [The ostracode biostratigraphy of the Antakya Basin]. *Geological Bulletin of Turkey* **36**, 115–137 [in Turkish with English abstract].
- SELÇUK, H. 1981. *Étude géologique de la partie meridionale du Hatay (Turquie)*. Doctoral Thesis, Université de Genève.
- TEMİZKAN, N. 2003. *Harbiye (Antakya) Civarının Jeolojik İncelemesi [Geological Investigation of the Harbiye (Antakya) Area]*. MSc Thesis, Çukurova University [in Turkish with English abstract, unpublished].
- YILMAZ, Y. 1982. *Amanos Dağlarının Tektoniği [Tectonics of the Amanos Mountains]*. TPAO (Turkish Petroleum Corporation) Report project number YDP-35 [in Turkish, unpublished].
- YILMAZ, Y., DEMİRKOL, C., YALÇIN, N., YETİŞ, C., YİĞİTBAŞ, E., GÜNAY, Y. & SARITAŞ B. 1984. *Amanos Dağlarının Jeolojisi [Geology of the Amanos Mountains]*. TPAO (Turkish Petroleum Corporation) Report no. 1920 [in Turkish, unpublished].

Received 02 January 2006; revised typescript received 05 December 2006; accepted 12 December 2006